Type VI secretion system killing by commensal *Neisseria* is influenced by the spatial dynamics of bacteria

Rafael Custodio, Rhian M. Ford[#], Cara J. Ellison, Guangyu Liu,

Gerda Mickute, Christoph M. Tang, and Rachel M. Exley[*]

Sir William Dunn School of Pathology,

University of Oxford,

South Parks Road,

Oxford OX1 3RE,

United Kingdom

#current address: Centre for Biomolecular Sciences, University of Nottingham, UK

[*]Correspondence: rachel.exley02@path.ox.ac.uk

ABSTRACT

Type VI Secretion Systems (T6SS) are widespread in bacteria and can dictate the development and organisation of polymicrobial ecosystems by mediating contact dependent killing. In *Neisseria* species, including *Neisseria cinerea* a commensal of the human respiratory tract, interbacterial contacts are mediated by Type four pili (Tfp) which promote formation of aggregates and govern the spatial dynamics of growing *Neisseria* microcolonies. Here we show that *N. cinerea* expresses a plasmid-encoded T6SS that is active and can limit growth of related pathogens. We explored the impact of Tfp expression on *N. cinerea* T6SS-dependent killing and show that expression of Tfp by prey strains enhances their susceptibility to T6SS, by keeping them in close proximity of T6SS-wielding attacker strains. Our findings have important implications for understanding how spatial constraints during contact-dependent antagonism can shape the evolution of microbial communities.

INTRODUCTION

The human microbiota is critical for the development of a healthy gastrointestinal immune system (Round and Mazmanian, 2009; Sommer and Bäckhed, 2013) and can also protect the host from invasion by pathogenic bacteria (Kamada et al., 2013). The microbes that carry out these important functions live as part of complex communities shaped by their fitness and ability to adapt to their environment, and which can be remodeled through mutualistic and antagonistic interactions (Garcia-Bayona and Comstock, 2018; Little et al., 2008; Nadell et al., 2016). Competition for niche and host-derived resources has therefore driven the evolution in bacteria of an array of mechanisms to suppress growth of, or kill neighbouring microbes. One mechanism, the Type VI Secretion System (T6SS), provides an effective strategy to eliminate competitors in a contact-dependent manner. The T6SS is a contractile, bacteriophage-like nanomachine that delivers toxins into the cytosol of target organisms (Cianfanelli et al., 2016; Ho et al., 2014). T6SS-associated effectors possess a broad range of activities, including nucleases (Koskiniemi et al., 2013; Ma et al., 2014; Pissaridou et al., 2018), phospholipases (Flaugnatti et al., 2016; Russell et al., 2013), peptidoglycan hydrolases (Whitney et al., 2013) and pore-forming proteins (Mariano et al., 2019); each effector is associated with a cognate immunity protein to prevent self-intoxication (Alcoforado Diniz et al., 2015; Unterweger et al., 2014). T6SSs have been best characterised in pathogenic bacteria, including *Pseudomonas*, *Vibrio*, *Salmonella* and *Shigella*, where its impact in pathogenesis and bacterial competition has been established *in vitro* and in some cases *in vivo* (Anderson et al., 2017; Sana et al., 2016). However, commensal bacteria also harbour T6SS, although how these systems combat pathogens has only been elucidated for *Bacteriodetes* in the intestinal tract (Russell et al., 2014); further studies are needed to gain

a greater appreciation of how T6SS in commensals influence microbial communities and pathogens in other niches.

The human nasopharynx hosts a polymicrobial community (Kumpitsch et al., 2019; Marchesi et al., 2017; Ramos-Sevillano et al., 2019), which can include the obligate human pathobiont *Neisseria meningitidis*, as well as related but generally non-pathogenic, commensal *Neisseria* species (Diallo et al., 2016; Dorey et al., 2019; Gold et al., 1978; Knapp and Hook, 1988; Sheikhi et al., 2015). *In vivo* studies have demonstrated an inverse relationship between carriage of commensal *Neisseria lactamica* and *N. meningitidis* (Deasy et al., 2015), while *in vitro* studies have revealed that some commensal *Neisseria* demonstrate potentially antagonistic effects against their pathogenic relatives (Custodio et al., 2020; Kim et al., 2019). Commensal and pathogenic *Neisseria* species have also been shown to interact closely in mixed populations (Custodio et al., 2020; Higashi et al., 2011a). Social interactions among *Neisseria* are mediated by surface structures known as Type IV pili (Tfp). These filamentous organelles enable pathogenic *Neisseria* to adhere to host cells (Nassif et al., 1993; Virji et al., 1991), and are crucial for microbe-microbe interactions and the formation of bacterial aggregates and microcolonies (Helaine et al., 2007; Higashi et al., 2007). In addition, Tfp interactions can dictate bacterial positioning within a community; non-piliated strains have been shown to be excluded to the expanding edge of colonies growing on solid media (Oldewurtel et al., 2015; Zöllner et al., 2017) while heterogeneity in pili, for example through post translational modifications, can alter how cells integrate into micocolonies (Zöllner et al., 2017).

We recently demonstrated that the pathogen *N. meningitidis* closely interacts with commensal *Neisseria cinerea* on human epithelial cell surfaces in a Tfp-dependent manner (Custodio et al., 2020). Here, whole genome sequence analysis revealed that the *N. cinerea* isolate used in our studies encodes a T6SS. We provide the first description of a functional T6SS in *Neisseria* spp.. We show that the *N. cinerea* T6SS is encoded on a plasmid and antagonises pathogenic relatives, *N. meningitidis* and *Neisseria gonorrhoeae*. Moreover, we examined whether Tfp influence the competitiveness of microbes in response to T6SS-mediated antagonism and demonstrate that T6SS–mediated competition is facilitated by Tfp in bacterial communities.

RESULTS

N. cinerea *346T encodes a functional T6SS on a plasmid*

We identified a single locus in *N. cinerea* isolate CCUG346T (346T) (https://www.ccug.se/strain?id=346) that encodes homologues of all 13 components that are necessary for a functional T6SS (Cascales and Cambillau, 2012), including genes predicted to encode canonical T6SS components Hcp and VgrG (**Figure 1A - table supplement 1**). We used T6SS-effector prediction software tools (Li et al., 2015) to search for putative effectors. In total we identified six putative effector and immunity genes, termed *Nte* and *Nti* for Neisseria T6SS effector/immunity, respectively. All Ntes contain a conserved Rhs domain, frequently associated with polymorphic toxins (Busby et al., 2013), and a variable C-terminal region. Nte1 contains an N-terminal PAAR motif, which can associate with the VgrG tip of T6SS (Shneider et al., 2013) and C-terminal phospholipase domain (cd00618). Nte2 also contains an N-terminal PAAR domain and has a predicted RNase domain (pfam15606) in its C-terminal region, while Nte3 is a putative HNH

endonuclease (pfam14411). Nte4 contains a GIY-YIG nuclease domain (cd00719) and Nte5 is predicted to be an HNH/endo VII nuclease (pfam14412), with Nte6 predicted to contain an HNHc endonuclease active site (cd00085).

Of note, all predicted T6SS-related *orf*s and Nte/Ntis in *N. cinerea* 346T were found to be encoded on a 108,141 bp plasmid, revealed by PacBio sequencing, and confirmed by PCR and sequencing. Nte/Nti 1-5 are encoded adjacent to the structural genes cluster, with Nte6/Nti6 encoded elsewhere in the plasmid (**Figure 1B - figure supplement 1**). Thus, our analysis reveals that the human commensal *N. cinerea* harbours a plasmid-borne T6SS together with six putative effector-immunity pairs.

Contraction of T6SSs leads to Hcp secretion, a hallmark of a functional T6SS (Cascales and Cambillau, 2012). Therefore, to establish whether the *N. cinerea* T6SS is functional, we assessed Hcp levels in whole cell lysates and supernatants from wild-type *N. cinerea*, a ΔT6SS mutant lacking 10 core genes including *hcp,* and a Δ*tssB* mutant. As expected, Hcp was detected in both fractions from the wild-type strain but not in cell lysates or supernatants from the ΔT6SS mutant (**Figure 1C**). Importantly, Hcp was present in cell lysates from the Δ*tssB* mutant, but not detected in cell supernatants, consistent with TssB being a component of the T6SS-tail-sheath required for contraction (Brackmann et al., 2018). Hcp secretion was restored by complementation of the Δ*tssB* mutant by chromosomal expression of TssB with a C-terminal sfGFP fusion (Δ*tssB*::*tssB*-sfGFP) (**Figure 1C**).

Next, we performed competition assays between *N. cinerea* 346T or the ΔT6SS mutant against *N. cinerea* 27178A which lacks a T6SS and Nte/Nti pairs identified in *N. cinerea* 346T. The survival of *N. cinerea* 27278A was reduced by around an order of magnitude following incubation with *N. cinerea* 346T compared with the ΔT6SS mutant (**Figure 1D**, $p < 0.0001$ and $p < 0.0001$, respectively), confirming that the *N. cinerea* 346T T6SS is active during inter-bacterial competition.

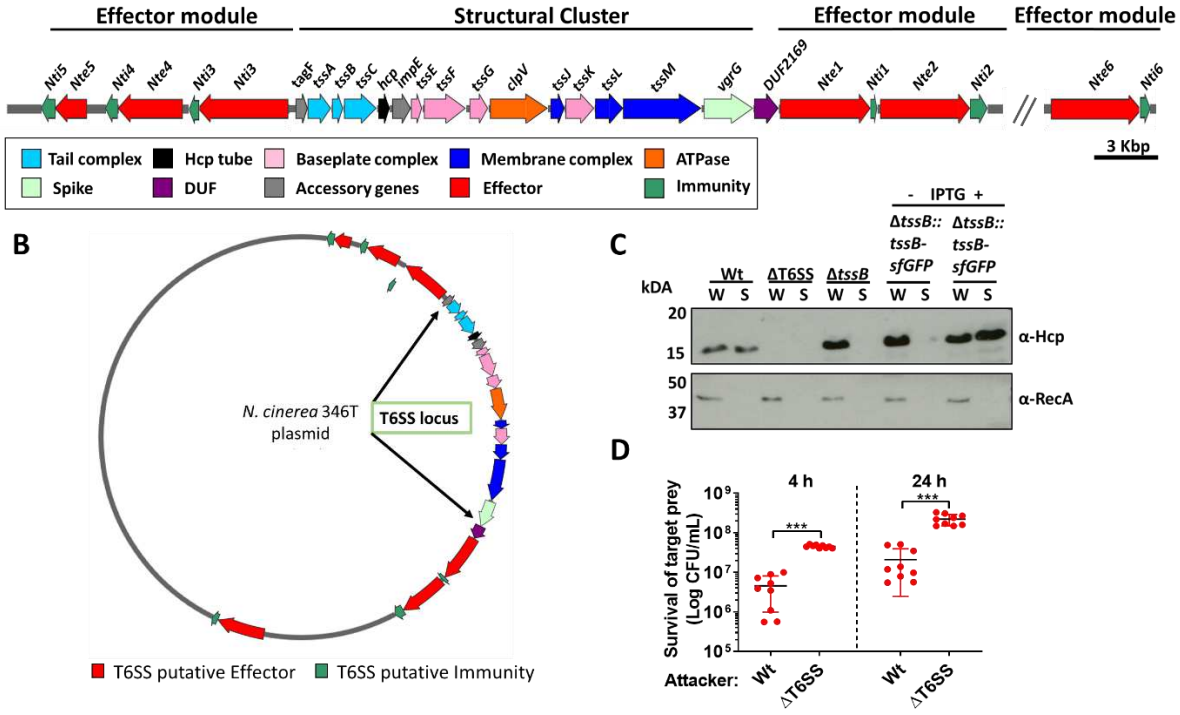

Figure 1. *N. cinerea* expresses a functional T6SS.

(A), Schematic representation of T6SS genes in *N. cinerea* 346T. Canonical *tss* nomenclature was used for genes in the T6SS cluster. **(B)** Map of the T6SS-associated genes encoded by the *N. cinerea* 346T plasmid. **(C)** Expression and secretion of Hcp by wild-type *N. cinerea* 346T (Wt) and the T6SS mutant (ΔT6SS). Hcp protein was detected in the whole cell lysates (W) and supernatants (S) by western blot analysis. For strain Δ*tssB*::*tssB*sfGFP, bacteria were grown in the presence (+) or absence (-) of 1 mM IPTG; molecular weight marker shown in

kDa. RecA is only detected in whole cell lysates. **(D)** Survival of the prey, *N. cinerea* 27178A, after 4 and 24 co-incubation with wild-type *N. cinerea* 346T or the T6SS mutant (ΔT6SS) at 10:1 ratio, attacker:prey. The mean ± SD of three independent experiments are shown: ***p < 0.0001 using unpaired two-tailed Student's t-test.

Dynamic behaviour of the* Neisseria *T6SS in the presence of prey cells

We further analysed the activity of the T6SS by visualising assembly and contraction in *N. cinerea* 346TΔ*tssB*::*tssB*-sfGFP; this strain exhibits comparable T6SS killing as wild-type *N. cinerea* 346T (**figure supplement 2**). Time-lapse microscopy revealed dynamic T6SS foci inside bacteria, with structures extending/contracting over seconds (**Figure 2A - movie supplement 1**) consistent with T6SS activity(Gerc et al., 2015; Ringel et al., 2017). To further confirm T6SS activity, we deleted the gene encoding the TssM homologue in strain 346TΔ*tssB*::*tssB*-sfGFP, abolishing T6SS activity (**Figure 2B**) and confirmed that in the absence of TssM, fluorescent structures were rarely seen (< 5% of cells in the Δ*tssM* background, compared with > 60% in the strain expressing TssM; **Figure 2C - movie supplement 2**).

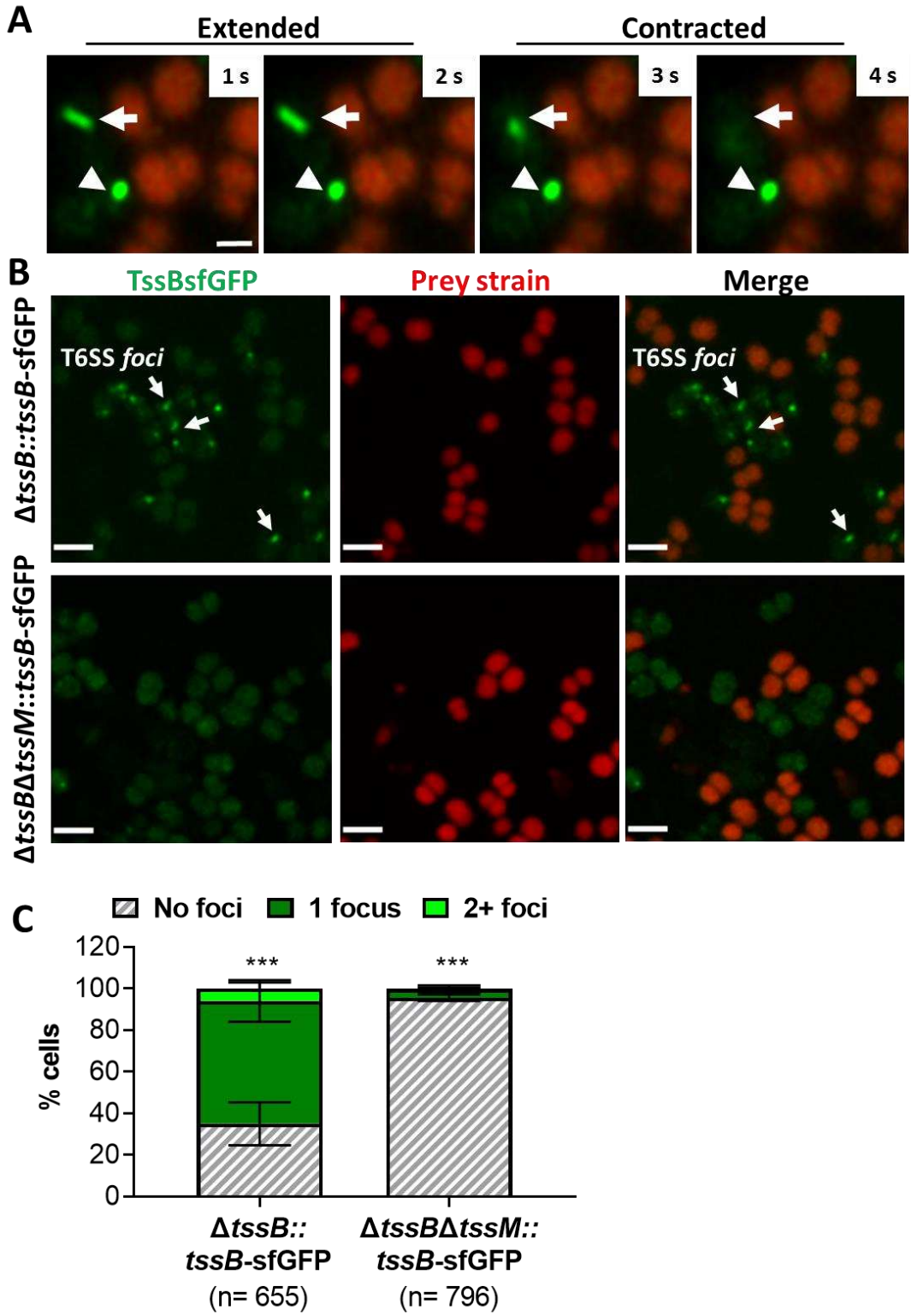

Figure 2. Visualisation of T6SS activity in *N. cinerea*.

(A) Assembly and contraction of the T6SS in *N. cinerea*; white arrows indicate contracting T6SSs. Time-lapse images of *N. cinerea* 346TΔ*tssB*::*tssB*sfGFP (green) and prey *N. cinerea*

27178A_ *sfCherry* (red); the arrowhead shows a non-dynamic focus, scale bar, 1 µm. See also Movie supplement 1. **(B)** Representative images of *N. cinerea* strains with the TssB::sfGFP fusion with (upper panels) or without (lower panels) TssM. Loss of fluorescent foci upon deletion of *tssM* indicates that foci correspond to active T6SS. The scale bar represents 2 µm. **(C)** Quantification of TssB-sfGFP foci in different strains. T6SS foci were quantified using 'analyse particle' (Fiji) followed by manual inspection. For each strain, at least two images from gel pads were obtained on two independent occasions. Percentage of cells with 0, 1, or 2+ foci are shown and n = number of cells analysed. Data shown are mean ± SD of two independent experiments: ***p<0.0001 using two-way ANOVA test for multiple comparison. See also Movie supplement 2.

Finally, we examined whether T6SS assembly induces lysis of prey cells. We imaged *N. cinerea* 346TΔ*tssB*::*tssB*-sfGFP with *N. cinerea* 27178 expressing sfCherry on gel pads with SYTOX Blue as an indicator of target cell permeability (Ringel et al., 2017). Interestingly, we detected increased SYTOX staining of prey cells immediately adjacent to predator bacteria displaying T6SS activity (**Figure 3 - movie supplement 3**), indicating that *N. cinerea* T6SS induces cell damage and lysis of its prey.

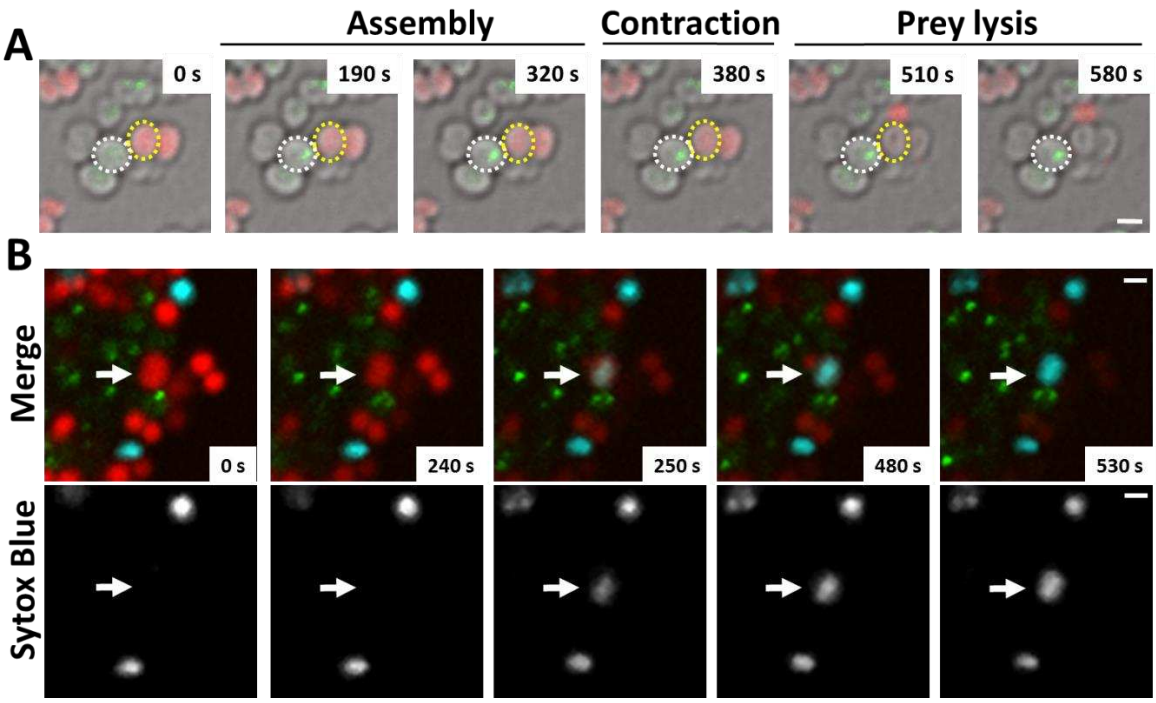

Figure 3. *N. cinerea* T6SS induces lysis in prey bacteria.

(A) Assembly of T6SS and prey lysis. Time-lapse series of merged images with phase contrast, *N. cinerea* 346T Δ*TssB*+*TssB*sfGFP (green), and *N. cinerea* 27178A sfCherry (red); scale bar, 1 µm. **(B)** Top row shows merged images of GFP (green, indicating T6SS assembly/contraction), mCherry (red, prey strain), and SYTOX Blue (cyan, showing membrane permeabilisation) channels. The bottom row arrows highlight a prey cell losing membrane integrity (increase in SYTOX Blue staining inside cells) arrows. Representative image from two biological repeats. Scale bars represent 1 µm. See also Movie supplement 3.

N. cinerea *T6SS effectors are functional toxin/immunity pairs*

To characterise the T6SS effector:immunity pairs, we expressed each Nte alone or with its corresponding Nti using an inducible expression plasmid in *E. coli*. We were only able to clone wild-type Nte6 in presence of its immunity protein, so Nte6^{R1300S} was used to analyse toxicity of this effector. In addition, as Nte1 encodes a predicted phospholipase that should

be active against cell membranes (Flaugnatti et al., 2016), we targeted the putative phospholipase domain of Nte1 to the periplasm by fusing it to the PelB signal sequence (Singh et al., 2013); cytoplasmic expression of the Nte1 phospholipase domain does not inhibit bacterial growth (**figure supplement 3**). All Ntes are toxic, with their expression leading to decreased viability and reduced optical density (OD) of *E. coli* cultures compared to empty vector controls; toxicity was counteracted by co-expression of the corresponding Nti (**Figure 4A-F**). Overall, these findings provide evidence that all six Nte/Ntis are effector-immunity proteins.

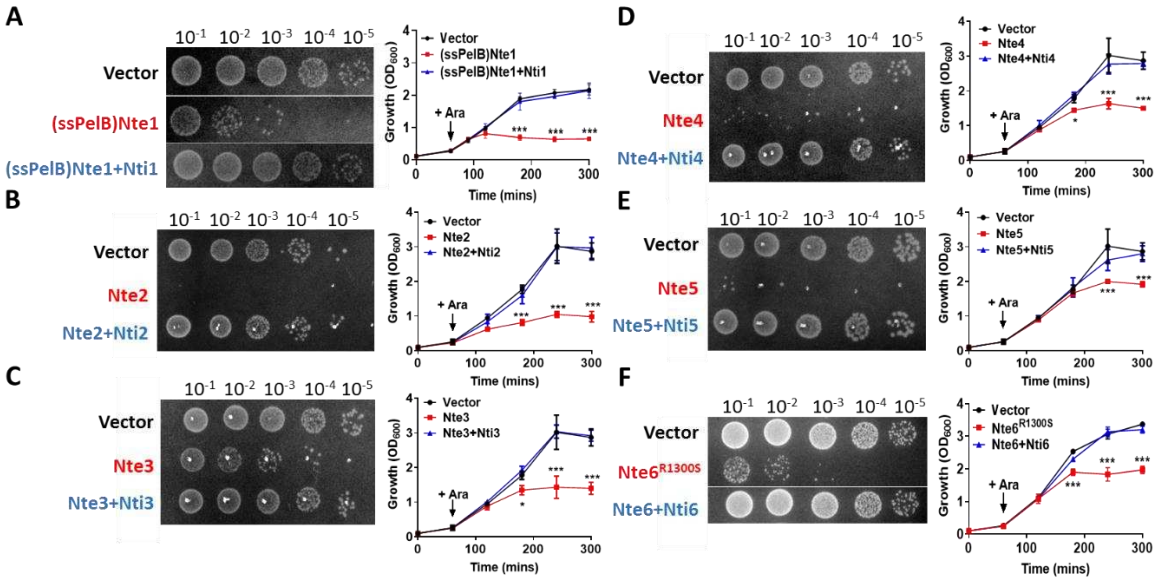

Figure 4. Putative *N. cinerea* T6SS effectors are toxic in *E. coli*.

(A) Arabinose (Ara) induced expression of T6SS effector Nte1 in periplasm of *E. coli* leads to reduction in CFU and OD at 600 nm (OD_{600}). Co-expression of putative immunity Nti1 restores growth to levels of strain with empty vector (pBAD33). **(B)-(E)** Cytoplasmic expression of putative effectors Nte2-5 without cognate immunity reduces growth and survival of *E. coli.* **(F)** Expression of $Nte6^{R1300S}$ reduces viability and growth when expressed in *E. coli*. Expression of Nti6 with Nte6 does not impact growth. In (A)-(F) number of CFU at 120 mins post induction are shown. Data shown are the mean ± SD of three independent

216 experiments: NS, not significant, ***p < 0.0001, *p < 0.05 using two-way ANOVA test for
217 multiple comparison. Images of colonies for Nte1 and Nte6 are composite as strains were
218 spotted to different areas of the same plates.
219
220 ***Commensal* Neisseria *T6SS kills human pathogens***
221 We next investigated whether commensal *N. cinerea* can deploy T6SS to antagonise the
222 related pathogenic species, *N. meningitidis* and *N. gonorrhoeae*. We performed competition
223 assays with three *N. meningitidis* strains (belonging to different lineages and expressing
224 different polysaccharide capsules *i.e.* serogroup B or C), and a strain of *N. gonorrhoeae*. *N.*
225 *cinerea* 346T caused between a 50 to 100-fold decrease in survival of the meningococcus
226 compared with the ΔT6SS strain, irrespective of lineage or serogroup (**Figure 5A**) and an
227 approximately 5-fold reduction is survival of the gonococcus (**Figure 5B**). We also
228 investigated whether the meningococcal capsule protects against T6SS assault. Using a
229 capsule-null strain (Δ*siaD*) in competition assays with wild-type *N. cinerea* 346T or the T6SS
230 mutant, we found there was an approximately 5-fold reduction in survival of the Δ*siaD*
231 mutant compared to the isogenic wild-type strain (**Figure 5C**). Therefore, the meningococcal
232 capsule protects bacteria against T6SS attack.
233

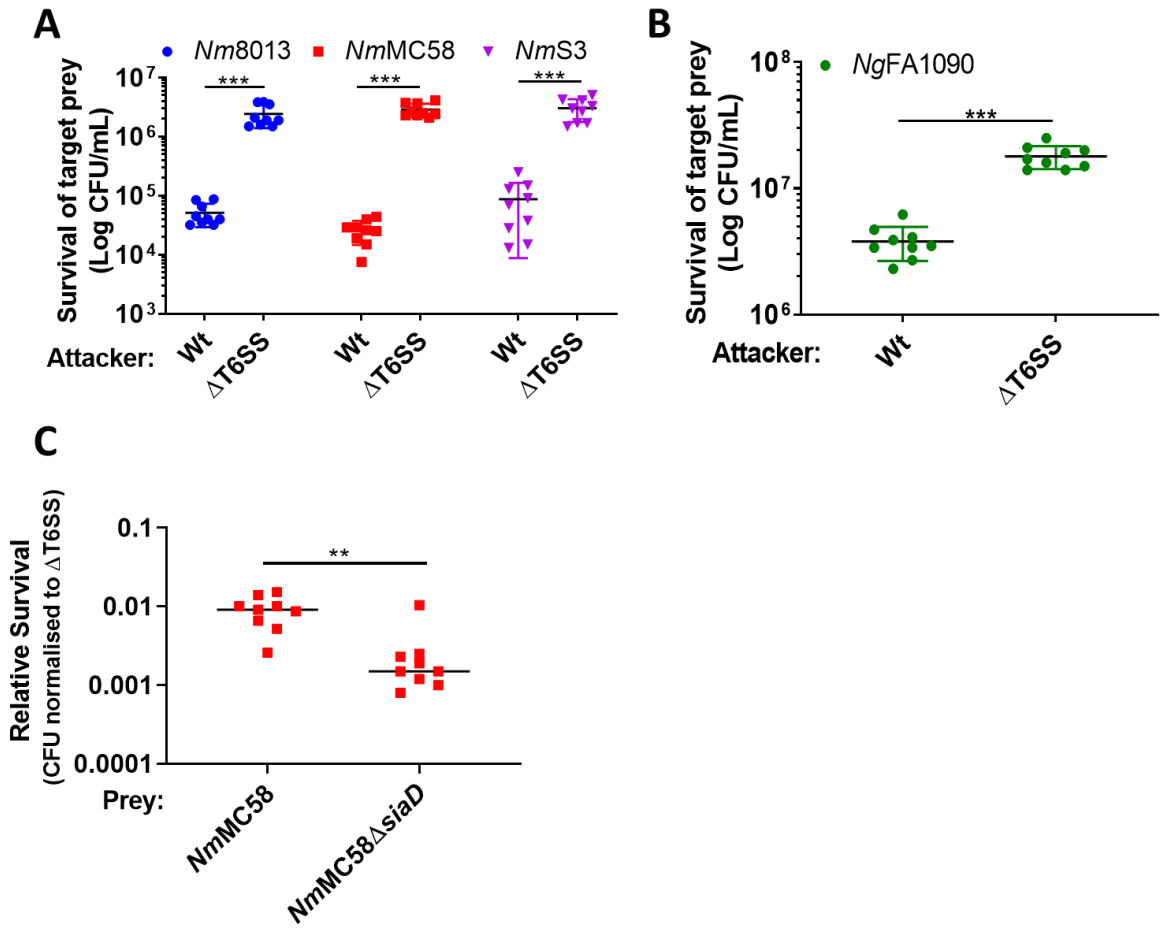

Figure 5: *N. cinerea* T6SS is active against pathogenic *N. meningitidis* and *N. gonorrhoeae*

(A) Recovery of wild-type *N. meningitidis* (*Nm*8013, *Nm*MC58, *Nm*S3) after 4 h co-incubation with *N. cinerea* 346T wild-type (Wt) or the T6SS mutant (ΔT6SS) at a 100:1 attacker:prey ratio. **(B)** Recovery of wild-type *N. gonorrhoeae* (FA1090) after 4 h co-incubation with *N. cinerea* 346T wild-type (Wt) or the T6SS mutant (ΔT6SS) at a 10:1 attacker:prey ratio, attacker:prey. **(C)** Unencapsulated *N. meningitidis* (*Nm*MC58Δ*siaD*) is more susceptible to T6SS-mediated killing than wild-type *N. meningitidis*. Recovery of *Nm*MC58 or the capsule-null mutant (*Nm*MC58Δ*siaD*) after 4 h co-culture with *N. cinerea* 346T (Wt) or a T6SS-deficient mutant (ΔT6SS) at ratio of 100:1, attacker:prey. Relative survival is defined as the fold change in recovery of *N. meningitidis* following incubation with wild-type *N. cinerea* compared to *N. cinerea* ΔT6SS. Data shown are the mean ± SD of three independent

246 experiments: NS, not significant, ***p < 0.0001, **p < 0.001 using unpaired two-tailed
247 Student's t-test for pairwise comparison (B and C) or one-way ANOVA test for multiple
248 comparison (A).
249
250 ***Spatial segregation driven by Type IV pili dictates prey survival against T6SS assault.***
251 Despite the potency of T6SS in *Neisseria* warfare, this nanomachine operates when bacteria
252 are in close proximity, so we hypothesised that Tfp, which are critical for the formation of
253 *Neisseria* microcolonies and organisation of bacterial communities (Higashi et al., 2007;
254 Mairey et al., 2006; Oldewurtel et al., 2015; Zöllner et al., 2017), could influence T6SS-
255 mediated antagonism. To test this we constructed fluorophore expressing, piliated and non-
256 piliated 'prey' strains (*i.e*. sfCherry-expressing 346TΔ*nte*/*i3-5* which is sensitive to T6SS-
257 mediated attack (**figure supplement 4**). Prey strains were mixed with piliated attacker strain
258 *N. cinerea* 346T expressing sfGFP at a 1:1 ratio on solid media, and the spatiotemporal
259 dynamics of bacterial growth examined by time-lapse stereo microscopy over 24 h, while
260 the relative proportion of each strain was analysed by flow cytometry at 24 h (**figure**
261 **supplement 5**). As expected based on previous observations of Tfp-mediated cell sorting in
262 *Neisseria* (Oldewurtel et al., 2015; Zöllner et al., 2017), the non-piliated prey strain
263 (346TΔ*nte*/*i3-5*Δ*pilE1*/*2_sfCherry*; red) segregates to the periphery of the colony, in this
264 location the prey strain escapes T6SS-mediated assault and dominates the expanding colony
265 (**Figure 6A - movie supplement 4 and figure supplement 5**). In contrast, when the prey is
266 piliated, pilus-mediated cell interactions prevent displacement of cells to the expanding
267 front (Oldewurtel et al., 2015; Ponisch et al., 2018; Zöllner et al., 2017), so the susceptible
268 strain (Tfp-expressing 346TΔ*nte*/*i3-5_sfCherry* Tfp+, red) is outcompeted by the T6SS+ strain
269 (Tfp-expressing 346T_*sfGfp* Tfp+, green) (**Figure 6B - movie supplement 5 and figure**

supplement 5). When both strains are piliated and immune to T6SS attack, there is no dominance of either strain (**Figure 6C - movie supplement 6 and figure supplement 5**). Assessment of the relative recovery of piliated and non-piliated prey in competition assays also supported the observation that the piliation status of the prey impacts survival against T6SS (**Figure 6D)**. These results highlight that, Tfp influence the outcome of T6SS-mediated antagonism through structuring and partitioning bacteria in mixed microcolonies.

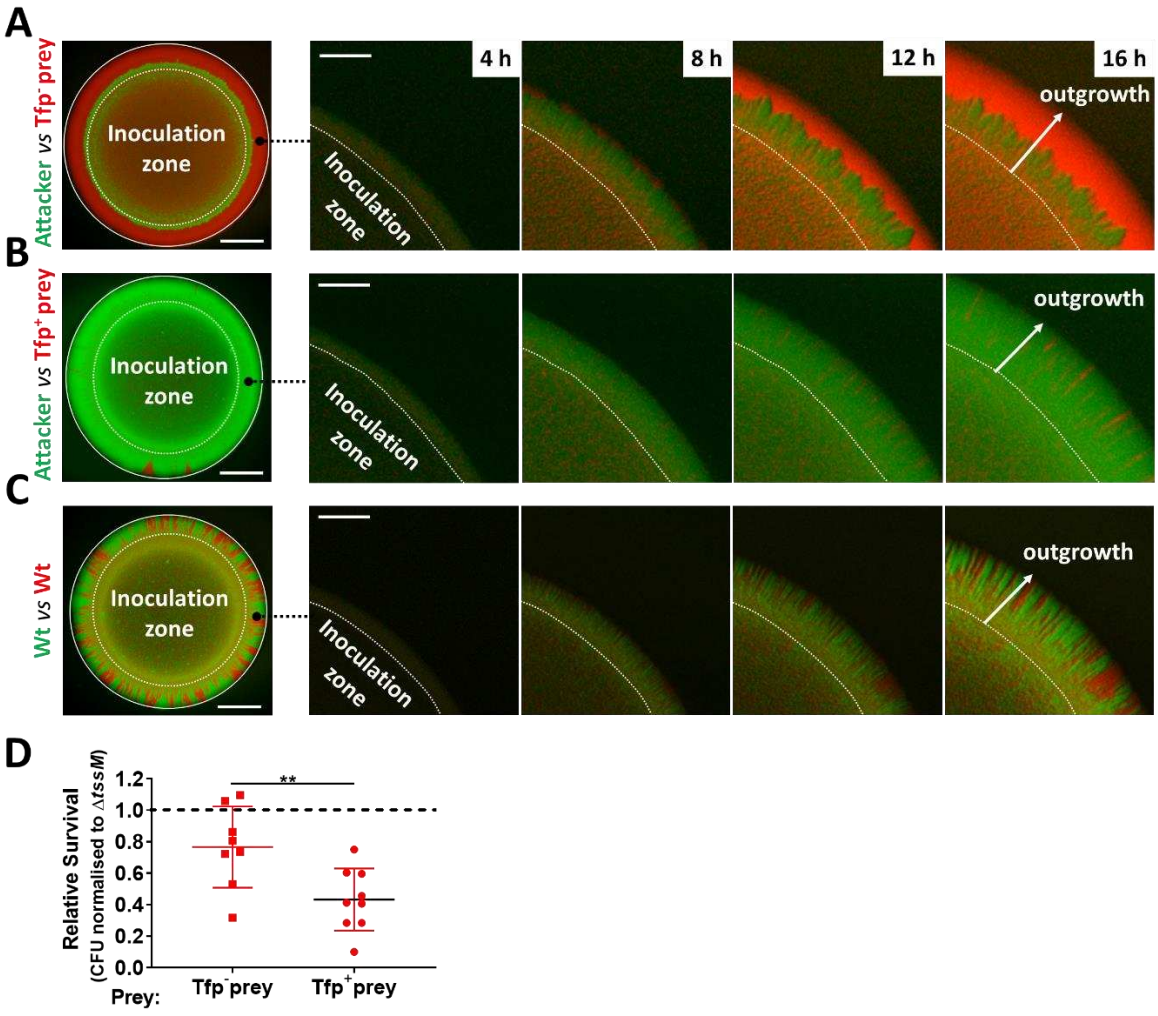

Figure 6: Predator and prey piliation promotes T6SS killing.

(A) Fluorescence microscopy images taken at specific times after inoculation of mixed (1:1 ratio) bacterial colonies. A T6SS-susceptible, non-piliated prey strain (346TΔ*nte*/*i3-5*Δ*pilE1/2_sfCherry*, red) migrates to the expanding edge of the colony over time,

281 segregating from the T6SS+ attacker strain (*N. cinerea* 346T_*gfp*, green) and dominating the
282 expanding population. **(B)** The same susceptible prey strain but expressing pili does not
283 segregate, and after 24h is outcompeted by the piliated T6SS+ attacker. **(C)** The non-T6SS-
284 susceptible piliated prey strain (346T_*sfCherry*, red) and piliated attacker strain (346T_sf*Gfp*,
285 green) do not segregate, but due to immunity against T6SS attack, no dominance is
286 observed. Images of colonies are representative of three independent experiments. Scale
287 bar, 500 µm. Expanding colony edge images are stills at indicated times from time-lapse
288 imaging performed on one occasion. Scale bar 100 µm. Movies supplement 4-6 show
289 expanding colonies in A-C, respectively. **(D)** The influence of piliation on T6SS killing.
290 Recovery of non-piliated and piliated prey strains after 24 h co-culture with *N. cinerea* 346T
291 (Wt) and a *tssM*-deficient mutant (Δ*tssM*) at ratio of 10:1, attacker:prey. Relative survival is
292 defined as the fold change in recovery of prey following incubation with wild-type attacker
293 *N. cinerea* compared to *N. cinerea* Δ*tssM*. Data shown are the mean ± SD of three
294 independent experiments: **p < 0.01 using unpaired two-tailed Student's t-test for pairwise
295 comparison.
296
297 **DISCUSSION**
298 Here we identified a T6SS in a commensal *Neisseria* spp. which can kill T6SS-deficient *N.*
299 *cinerea* isolates and the related pathogens, *N. meningitidis*, with which it shares an
300 ecological niche (Knapp and Hook, 1988), and *N. gonorrhoeae*. Of note, the *N. cinerea* T6SS
301 is encoded on a large plasmid, with structural genes for the single T6SS apparatus clustered
302 in one locus, similar to other T6SS (Anderson et al., 2017; Liaw et al., 2019; Sana et al.,
303 2016). Effectors Nte1 to 5 are also encoded in the same locus, but with Nte6 encoded
304 elsewhere on the plasmid. To date, plasmid encoded T6SS have only been described in

Campylobacter species (Marasini and Fakhr, 2016), with this plasmid T6SS mobilised *via* conjugation (Marasini et al., 2020). Although other small plasmids have been reported in *N. cinerea* (Knapp et al., 1984; Roberts, 1989) and *N. cinerea* can be a recipient of *N. gonorrhoeae* plasmids (Genco et al., 1984), it is not yet known whether T6SS plasmids are widespread among *Neisseria*, or whether the plasmid can be mobilised by conjugation or transformation. Interestingly, in *Acinetobacter baylyi*, T6SS induced prey cell lysis contributes to acquisition of plasmids from target cells (Ringel et al., 2017). Therefore, it will be interesting to see whether other *Neisseria* species with T6SS genes (Marri et al., 2010) harbour T6SS-expressing plasmids.

Examination of *N. cinerea* T6SS activity revealed several interesting features. Microscopy demonstrated that T6SS attack (tit-for-tat) is not required to provoke firing of the system. Instead, the T6SS appears to be constitutively active in *N. cinerea* (**Figure 2**). Furthermore, the system is capable of inducing lysis of prey bacteria (**Figure 3**). The consequences of T6SS attack are determined by the repertoire and activities of effectors, and their site of delivery. Many different effector activities have been proposed including lipases, peptidoglycan hydrolases, metalloproteases and nucleases (Lewis et al., 2019). Effector activities can result in target cell lysis to varying degrees (Ringel et al., 2017; Smith et al., 2020). Of the six Ntes we identified, lysis could be mediated by Nte1 which harbours a putative phospholipase domain in the C-terminus. Alternatively, a combination of effectors might be needed to elicit prey lysis.

Polysaccharide capsules are largely thought to provide bacteria with a strategy for evading host immune killing (Lewis and Ram, 2014). Here, we found that the meningococcal capsule

329 has an alternative role in defence against other bacteria. Meningococcal strains lacking a
330 capsule were at a significant disadvantage in the face of a T6SS-expressing competitor
331 implicating this surface polysaccharide in protection against T6SS assault. Similar findings
332 have been reported for other bacteria; for example the extracellular polysaccharide of *V.*
333 *cholerae* and the colonic acid capsule of *E. coli* confer defence against T6SS attack (Hersch et
334 al., 2020; Toska et al., 2018). One potential mechanism is that the capsule sterically impairs
335 the ability of the T6SS to penetrate the target cell membrane, and/or inhibits access of T6SS
336 effectors to their cellular targets. Interestingly, recent genetic evidence indicates that some
337 commensal *Neisseria* species also have capacity to produce polysaccharide capsules
338 (Clemence et al., 2018), which might also confer a survival advantage in mixed populations
339 that include strains expressing T6SS.
340
341 Most bacteria exist within complex polymicrobial communities in which the spatial and
342 temporal dynamics of proliferation and death has a major effect on their fitness and survival
343 (Nadell et al., 2016). While structured complex microbial societies can benefit all their
344 members (Gabrilska and Rumbaugh, 2015; Wolcott et al., 2013), antagonistic neighbours,
345 especially those deploying contact-dependent killing mechanisms, can disrupt communities.
346 Although T6SS-mediated killing can be advantageous to a producing strain during bacterial
347 competition, this requires intimate association with its prey (MacIntyre et al., 2010; Russell
348 et al., 2014). Thus, one way for susceptible bacteria to evade T6SS killing is to avoid direct
349 contact with attacking cells (Borenstein et al., 2015; Smith et al., 2020). In *Neisseria*, the Tfp
350 is a key mediator of interbacterial and interspecies interactions (Custodio et al., 2020;
351 Higashi et al., 2011b) and pilus-mediated interactions influence the spatial structure of a
352 growing community (Oldewurtel et al., 2015; Zöllner et al., 2017). In *N. gonorrhoeae,* non-

353 piliated bacteria segregate to the expanding front of the colony and Tfp-mediated spatial
354 reorganisation can allow bacteria to avoid external stresses or strains competing for
355 resources (Oldewurtel et al., 2015; Zöllner et al., 2017). We predicted that this would be
356 especially relevant in the context of T6SS mediated antagonism, where physical exclusion
357 driven by Tfp-loss or modification, which may occur naturally in a polymicrobial
358 environment and is an established phenomenon in pathogenic *Neisseria* (Hagblom et al.,
359 1985; Helm and Seifert, 2010), could be an effective strategy to evade and survive an
360 antagonistic interaction, while pilus-mediated interactions might be less favourable for a
361 susceptible prey. Our results demonstrate that piliation of the predator and prey strains of
362 *N. cinerea* led to dominance of the T6SS-expressing strain, indicating that *N. cinerea* Tfp
363 amplify T6SS-mediated competition. It is noteworthy that many bacteria (*e.g. Pseudomonas*
364 *aeruginosa*, *Vibrio cholerae*, *Acinetobacter baumannii*, enteropathogenic *E. coli*) that employ
365 T6SS for inter-bacterial competition also express Tfp. Therefore, our findings are of broad
366 relevance for the impact of contact dependent killing, and further emphasise how precise
367 spatial relationships can have profound effects on how antagonistic and mutualistic factors
368 combine to influence the development of microbial communities.
369

370 **MATERIALS AND METHODS**

371

372 ***Bacterial strains and growth***

373 Bacterial strains used in this study are shown in **Table Supplement 2**. *Neisseria* spp. were
374 grown on Brain Heart Infusion (BHI, Oxoid) agar with 5% defibrinated horse blood or in BHI
375 broth at 37°C with 5% CO_2 or GC-medium supplemented with 1.5% base agar (w/v) and 1%
376 Vitox (v/v; Oxoid). GW-medium (Wade and Graver, 2007) was used for *N. cinerea*

microscopy experiments. *E. coli* was grown on LB (Lennox Broth base, Invitrogen) agar or in liquid LB at 37°C with shaking. Antibiotics were added at the following concentrations: for *E. coli*, carbenicillin (carb) 100 µg/ml, kanamycin (kan) 50 µg/ml, and chloramphenicol (cm) 20 µg/ml; for *Neisseria* spp. kan 75 µg/ml, spectinomycin (spec) 65 µg/ml, erythromycin (ery) 15 µg/ml, and polymyxin B (pmB) 10 µg/ml.

DNA Isolation and whole-genome sequencing (WGS)

Genomic DNA was extracted using the Wizard Genomic Kit (Promega), and sequenced by PacBio (Earlham Institute, Norwich) using single-molecule real-time (SMRT) technology; reads were assembled *de novo* with HGAP3(Chin et al., 2013).

Construction of* N. cinerea *mutants

Primers used in this study are listed in **Table supplement 3**. Target genes were replaced with antibiotic cassettes as previously (Wörmann et al., 2016). Constructs were assembled into pUC19 by Gibson Assembly (New England Biolabs), and hosted in *Escherichia coli* DH5α. Plasmids were linearised with *Sca*I, and gel extracted relevant linearised fragments used to transform *N. cinerea*; transformants were checked by PCR and sequencing.

Complementation or chromosomal insertion of genes encoding fluorophores was achieved using pNCC1-Spec, a spectinomycin-resistant derivative of pNCC1(Wörmann et al., 2016). For visualisation of T6SS-sheaths, *sfgfp* was cloned in-frame with *tssB* and a short linker (encoding 3×Ala 3×Gly) by Gibson Assembly (New England Biolabs) into pNCC1-Spec to allow IPTG-inducible expression of TssB-sfGFP. PCR was performed using Herculase II (Agilent) or Q5 High-fidelity DNA Polymerase (New England Biolabs).

401 ***Analysis of effector/immunity activity in E. coli***

402 Putative effector coding sequences with or without cognate immunity gene were amplified
403 by PCR from *N. cinerea* 346T gDNA and either assembled by Gibson Assembly (NEB) into
404 pBAD33 or, for Nte1 with or without addition of the PelB signal sequence, cloned in to
405 pBAD33 using XbaI / SphI restriction enzyme sites. Plasmids were transformed into *E. coli*
406 DH5α and verified by sequencing (Source Bioscience). For assessment of toxicity, strains
407 with recombinant or empty pBAD33 plasmids were grown overnight in LB supplemented
408 with 0.8% glucose (w/v), then diluted to an OD_{600} of 0.1 and incubated for 1 hour at 180 rpm
409 and 37°C; bacteria were pelleted and resuspended in LB with arabinose (0.8% w/v) to induce
410 expression and incubated at 37°C, 180 rpm for a further 4 h. The OD_{600} and CFU/ml of
411 cultures were determined; aliquots were diluted and plated to media containing 0.8%
412 glucose at relevant time points up to 5 h.

413

414 ***Hcp protein expression, purification and antibody generation***

415 Codon optimised *hcp* was synthesised with a sequence encoding an N-terminal 6x His Tag
416 and a 3C protease cleavage site, and flanked by *Nco*I and *Xho*I restriction sites
417 (ThermoFisher). The fragment was ligated into *Nco*I and *Xho*I sites in pET28a (Novagen)
418 using QuickStick T4 DNA Ligase (Bioline) and transformed into *E. coli* B834. Bacteria were
419 grown at 37°C, 150 rpm to an OD_{600} of 1.0, and expression of 6xHis-3C-Hcp was induced with
420 1 mM IPTG for 24 h at 16°C. Cells were resuspended in Buffer A (50 mM Tris-HCl buffer pH
421 7.5, 10 mM Imidazole, 500 mM NaCl, 1 mM DTT) containing protease inhibitors, 1 mg/mL
422 lysozyme and 100 µg/mL DNase then subsequently homogenised with an EmulsiFlex-C5
423 (Avestin). Lysed cells were ultracentrifuged and the cleared supernatant loaded onto a Ni
424 Sepharose 6 Fast Flow His Trap column (GE Healthcare) equilibrated with Buffer A. The

column was washed with Buffer A, then Buffer B (50 mM Tris-HCl buffer pH 7.5, 35 mM Imidazole, 500 mM NaCl, 1 mM DTT) before elution with 10 mL of Buffer C (50 mM Tris-HCl buffer pH 7.5, 300 mM Imidazole, 150 mM NaCl, 1 mM DTT). The eluate was incubated with the HRV-3C protease (Sigma) then applied to a Ni Sepharose column. The eluate containing protease and cleaved protein was concentrated using Amicon Ultra 10,000 MWCO (Millipore), then passed through a Superdex-200 column (GE Healthcare, Buckinghamshire, UK). Fractions were analysed by SDS-PAGE and Coomassie blue staining, and those with Hcp pooled and used to generate polyclonal antibodies (EuroGentec).

Hcp secretion assay

Bacteria were grown in BHI broth for 4-5 h then harvested and lysed in an equal volume of SDS-PAGE lysis buffer (500 mM Tris-HCl [pH 6.8], 5% SDS, 15% glycerol, 0.5% bromophenol blue containing 100 mM β-mercaptoethanol); supernatants were filtered (0.22 µm pore, Millipore) and proteins precipitated with 20% (v/v) trichloroacetic acid. Hcp was detected by Western blot with anti-Hcp (1:10,000 dilution) and goat anti-rabbit IgG–HRP (1:5000, sc-2004; Santa Cruz). Anti-RecA (1:5000 dilution, ab63797; Abcam) followed by goat anti-rabbit IgG–HRP and detection with ECL detection Reagent (GE Healthcare) or Coomassie blue staining were used as loading controls.

Live cell imaging of T6SS activity

Bacteria were grown overnight on BHI agar, resuspended in PBS and 20 µl spotted onto fresh BHI agar containing 1 mM IPTG and incubated for 4 h at 37°C. After incubation, 500 µl of 10^9 cfu/mL bacterial suspension of attacker was mixed with the prey strain at a 1:1 ratio.

Cells were harvested by centrifugation for 3 min at 6000 rpm, resuspended in 100 µL of PBS or GW media and 2 µl spotted on 1% agarose pads (for T6SS dynamics) or GW media with 0.1 mM IPTG and 0.5 µM SYTOX™Blue (Thermo Fisher Scientific) for assessment of prey permeability. Fluorescence microscopy image sequences were acquired within 20-30 minutes of sample preparation with an inverted Zeiss 880 Airyscan microscope equipped with Plan-Apochromat 63×/1.4-NA oil lens and fitted with a climate chamber mounted around the objective to perform the imaging at 37°C with 5% CO_2. Automated images were collected at 1 sec, 10 sec or 1 min intervals and processed with Fiji (Schindelin et al., 2012). Background noise was reduced using the "Despeckle" filter. The XY drift was corrected using StackReg with "Rigid Body" transformation (Thévenaz et al., 1998). Experiments and imaging were performed on at least two independent occasions.

Quantitative competition assays

Strains grown overnight on BHI agar were resuspended in PBS and diluted to 10^9 CFU/mL, mixed at the indicated ratio, then 20 µl spotted onto BHI agar in triplicate and incubated at 37°C with 5% CO_2. At specific time-points, entire spots were harvested and resuspended in 1 mL of PBS. The cellular suspension was then serially diluted in PBS and aliquots spotted onto selective media. Colonies were counted after ~16 h incubation at 37 °C with 5% CO_2. Experiments were performed on at least three independent occasions. For different prey analysis relative survival was defined as the fold change in recovery of prey following incubation with wild-type attacker *N. cinerea* compared to a T6SS-deficient *N. cinerea*.

Competition assays assessed by Fluorescence microscopy and flow cytometry

Bacteria were prepared and grown as described for quantitative competition assays except using 1 µl spot volume and spotted onto GC-medium supplemented with 0.5% base agar (w/v) and 1% Vitox (v/v; Oxoid). At various time points expanding colonies were imaged using a M125C stereo microscope equipped with a DFC310FX digital camera (Leica Microsystems) and images processed with Fiji. Images were imported using "Image Sequence" and corrected with StackReg as described. For flow cytometry, colonies were harvested, fixed with 4% PFA for 20 min then washed with PBS. Samples were analysed using a Cytoflex LX (Beckman Coulter), and at least 10^4 events recorded. Fluorescence, forward and side scatter data were collected to distinguish between debris and bacteria. Results were analysed by calculating the number of events positive for either GFP or Cherry signal in FlowJo v10 software (Becton Dickinson Company). Events that were negative for fluorescence or positive for both markers were also plotted. Flow cytometry analysis was performed on two independent occasions. Stereo microscopy analysis was performed on three independent occasions with technical duplicates each time.

Statistical analyses

Graphpad Prism7 software (San Diego, CA) was used for statistical analysis. We used One-way/two-way ANOVA with Tukey post hoc testing for multiple comparisons and unpaired two-tailed Student's t-test for pairwise comparisons. In all cases, $p < 0.05$ was considered statistically significant.

ACKNOWLEDGEMENTS

We thank members of the Foster group (Oxford) especially Daniel Unterweger (now at the University of Kiel) for advice and assistance with microscopy as well as Alan Wainman of the

SWDSP Bioimaging facility. We are grateful to M. Basler (Basel) for valuable advice, and to Meningitis Now for funding. Work in CMT's lab is supported by a Wellcome Trust Investigator award (102908/Z/13/Z).

COMPETING INTERESTS

The authors declare no competing interests.

REFERENCES

Alcoforado Diniz, J., Liu, Y.C., and Coulthurst, S.J. (2015). Molecular weaponry: diverse effectors delivered by the Type VI secretion system. Cellular microbiology *17*, 1742-1751.

Anderson, M.C., Vonaesch, P., Saffarian, A., Marteyn, B.S., and Sansonetti, P.J. (2017). Shigella sonnei Encodes a Functional T6SS Used for Interbacterial Competition and Niche Occupancy. Cell host & microbe *21*, 769-776.e763.

Borenstein, D.B., Ringel, P., Basler, M., and Wingreen, N.S. (2015). Established Microbial Colonies Can Survive Type VI Secretion Assault. PLoS computational biology *11*, e1004520.

Brackmann, M., Wang, J., and Basler, M. (2018). Type VI secretion system sheath inter-subunit interactions modulate its contraction. EMBO reports *19*, 225-233.

Busby, J.N., Panjikar, S., Landsberg, M.J., Hurst, M.R., and Lott, J.S. (2013). The BC component of ABC toxins is an RHS-repeat-containing protein encapsulation device. Nature *501*, 547-550.

Cascales, E., and Cambillau, C. (2012). Structural biology of type VI secretion systems. Philos Trans R Soc Lond B Biol Sci *367*, 1102-1111.

Chin, C.S., Alexander, D.H., Marks, P., Klammer, A.A., Drake, J., Heiner, C., Clum, A., Copeland, A., Huddleston, J., Eichler, E.E., *et al.* (2013). Nonhybrid, finished microbial genome assemblies from long-read SMRT sequencing data. Nature methods *10*, 563-569.

520 Cianfanelli, F.R., Monlezun, L., and Coulthurst, S.J. (2016). Aim, Load, Fire: The Type VI
521 Secretion System, a Bacterial Nanoweapon. Trends in microbiology *24*, 51-62.
522 Clemence, M.E.A., Maiden, M.C.J., and Harrison, O.B. (2018). Characterization of capsule
523 genes in non-pathogenic Neisseria species. Microb Genom *4*.
524 Custodio, R., Johnson, E., Liu, G., Tang, C.M., and Exley, R.M. (2020). Commensal Neisseria
525 cinerea impairs Neisseria meningitidis microcolony development and reduces pathogen
526 colonisation of epithelial cells. PLoS pathogens *16*, e1008372.
527 Deasy, A.M., Guccione, E., Dale, A.P., Andrews, N., Evans, C.M., Bennett, J.S., Bratcher, H.B.,
528 Maiden, M.C., Gorringe, A.R., and Read, R.C. (2015). Nasal Inoculation of the Commensal
529 Neisseria lactamica Inhibits Carriage of Neisseria meningitidis by Young Adults: A Controlled
530 Human Infection Study. Clinical infectious diseases : an official publication of the Infectious
531 Diseases Society of America *60*, 1512-1520.
532 Diallo, K., Trotter, C., Timbine, Y., Tamboura, B., Sow, S.O., Issaka, B., Dano, I.D., Collard, J.M.,
533 Dieng, M., Diallo, A.*, et al.* (2016). Pharyngeal carriage of Neisseria species in the African
534 meningitis belt. The Journal of infection *72*, 667-677.
535 Dorey, R.B., Theodosiou, A.A., Read, R.C., and Jones, C.E. (2019). The nonpathogenic
536 commensal Neisseria: friends and foes in infectious disease. Curr Opin Infect Dis *32*, 490-496.
537 Flaugnatti, N., Le, T.T., Canaan, S., Aschtgen, M.S., Nguyen, V.S., Blangy, S., Kellenberger, C.,
538 Roussel, A., Cambillau, C., Cascales, E.*, et al.* (2016). A phospholipase A1 antibacterial Type VI
539 secretion effector interacts directly with the C-terminal domain of the VgrG spike protein for
540 delivery. Molecular microbiology *99*, 1099-1118.
541 Gabrilska, R.A., and Rumbaugh, K.P. (2015). Biofilm models of polymicrobial infection. Future
542 microbiology *10*, 1997-2015.

543 Garcia-Bayona, L., and Comstock, L.E. (2018). Bacterial antagonism in host-associated
544 microbial communities. Science (New York, NY) *361*.
545 Genco, C.A., Knapp, J.S., and Clark, V.L. (1984). Conjugation of plasmids of Neisseria
546 gonorrhoeae to other Neisseria species: potential reservoirs for the beta-lactamase plasmid.
547 J Infect Dis *150*, 397-401.
548 Gerc, A.J., Diepold, A., Trunk, K., Porter, M., Rickman, C., Armitage, J.P., Stanley-Wall, N.R.,
549 and Coulthurst, S.J. (2015). Visualization of the Serratia Type VI Secretion System Reveals
550 Unprovoked Attacks and Dynamic Assembly. Cell reports *12*, 2131-2142.
551 Gold, R., Goldschneider, I., Lepow, M.L., Draper, T.F., and Randolph, M. (1978). Carriage of
552 Neisseria meningitidis and Neisseria lactamica in infants and children. J Infect Dis *137*, 112-
553 121.
554 Hagblom, P., Segal, E., Billyard, E., and So, M. (1985). Intragenic recombination leads to pilus
555 antigenic variation in Neisseria gonorrhoeae. Nature *315*, 156-158.
556 Helaine, S., Dyer, D.H., Nassif, X., Pelicic, V., and Forest, K.T. (2007). 3D structure/function
557 analysis of PilX reveals how minor pilins can modulate the virulence properties of type IV pili.
558 Proceedings of the National Academy of Sciences of the United States of America *104*, 15888-
559 15893.
560 Helm, R.A., and Seifert, H.S. (2010). Frequency and rate of pilin antigenic variation of Neisseria
561 meningitidis. J Bacteriol *192*, 3822-3823.
562 Hersch, S.J., Watanabe, N., Stietz, M.S., Manera, K., Kamal, F., Burkinshaw, B., Lam, L., Pun,
563 A., Li, M., Savchenko, A.*, et al.* (2020). Envelope stress responses defend against type six
564 secretion system attacks independently of immunity proteins. Nature microbiology *5*, 706-
565 714.

566 Higashi, D.L., Biais, N., Weyand, N.J., Agellon, A., Sisko, J.L., Brown, L.M., and So, M. (2011a).
567 N. elongata produces type IV pili that mediate interspecies gene transfer with N.
568 gonorrhoeae. PLoS One *6*, e21373.
569 Higashi, D.L., Biais, N., Weyand, N.J., Agellon, A., Sisko, J.L., Brown, L.M., and So, M. (2011b).
570 N. elongata Produces Type IV Pili That Mediate Interspecies Gene Transfer with N.
571 gonorrhoeae. Plos One *6*.
572 Higashi, D.L., Lee, S.W., Snyder, A., Weyand, N.J., Bakke, A., and So, M. (2007). Dynamics of
573 Neisseria gonorrhoeae attachment: Microcolony development, cortical plaque formation,
574 and cytoprotection. Infection and immunity *75*, 4743-4753.
575 Ho, B.T., Dong, T.G., and Mekalanos, J.J. (2014). A view to a kill: the bacterial type VI secretion
576 system. Cell host & microbe *15*, 9-21.
577 Kamada, N., Chen, G.Y., Inohara, N., and Núñez, G. (2013). Control of pathogens and
578 pathobionts by the gut microbiota. Nature immunology *14*, 685-690.
579 Kim, W.J., Higashi, D., Goytia, M., Rendón, M.A., Pilligua-Lucas, M., Bronnimann, M., McLean,
580 J.A., Duncan, J., Trees, D., Jerse, A.E.*, et al.* (2019). Commensal Neisseria Kill Neisseria
581 gonorrhoeae through a DNA-Dependent Mechanism. Cell host & microbe *26*, 228-239.e228.
582 Knapp, J.S., and Hook, E.W., 3rd (1988). Prevalence and persistence of Neisseria cinerea and
583 other Neisseria spp. in adults. J Clin Microbiol *26*, 896-900.
584 Knapp, J.S., Totten, P.A., Mulks, M.H., and Minshew, B.H. (1984). Characterization of Neisseria
585 cinerea, a nonpathogenic species isolated on Martin-Lewis medium selective for pathogenic
586 Neisseria spp. J Clin Microbiol *19*, 63-67.
587 Koskiniemi, S., Lamoureux, J.G., Nikolakakis, K.C., t'Kint de Roodenbeke, C., Kaplan, M.D., Low,
588 D.A., and Hayes, C.S. (2013). Rhs proteins from diverse bacteria mediate intercellular

competition. Proceedings of the National Academy of Sciences of the United States of America *110*, 7032-7037.

Kumpitsch, C., Koskinen, K., Schopf, V., and Moissl-Eichinger, C. (2019). The microbiome of the upper respiratory tract in health and disease. BMC Biol *17*, 87.

Lewis, J.M., Deveson Lucas, D., Harper, M., and Boyce, J.D. (2019). Systematic Identification and Analysis of Acinetobacter baumannii Type VI Secretion System Effector and Immunity Components. Frontiers in microbiology *10*, 2440.

Lewis, L.A., and Ram, S. (2014). Meningococcal disease and the complement system. Virulence *5*, 98-126.

Li, J., Yao, Y., Xu, H.H., Hao, L., Deng, Z., Rajakumar, K., and Ou, H.Y. (2015). SecReT6: a web-based resource for type VI secretion systems found in bacteria. Environmental microbiology *17*, 2196-2202.

Liaw, J., Hong, G., Davies, C., Elmi, A., Sima, F., Stratakos, A., Stef, L., Pet, I., Hachani, A., Corcionivoschi, N.*, et al.* (2019). The Campylobacter jejuni Type VI Secretion System Enhances the Oxidative Stress Response and Host Colonization. Frontiers in microbiology *10*, 2864.

Little, A.E.F., Robinson, C.J., Peterson, S.B., Raffa, K.E., and Handelsman, J. (2008). Rules of Engagement: Interspecies Interactions that Regulate Microbial Communities. Annu Rev Microbiol *62*, 375-401.

Ma, L.S., Hachani, A., Lin, J.S., Filloux, A., and Lai, E.M. (2014). Agrobacterium tumefaciens deploys a superfamily of type VI secretion DNase effectors as weapons for interbacterial competition in planta. Cell host & microbe *16*, 94-104.

MacIntyre, D.L., Miyata, S.T., Kitaoka, M., and Pukatzki, S. (2010). The Vibrio cholerae type VI secretion system displays antimicrobial properties. Proceedings of the National Academy of Sciences of the United States of America *107*, 19520-19524.

613 Mairey, E., Genovesio, A., Donnadieu, E., Bernard, C., Jaubert, F., Pinard, E., Seylaz, J., Olivo-
614 Marin, J.C., Nassif, X., and Dumenil, G. (2006). Cerebral microcirculation shear stress levels
615 determine Neisseria meningitidis attachment sites along the blood-brain barrier. J Exp Med
616 *203*, 1939-1950.
617 Marasini, D., and Fakhr, M.K. (2016). Complete Genome Sequences of Campylobacter jejuni
618 Strains OD267 and WP2202 Isolated from Retail Chicken Livers and Gizzards Reveal the
619 Presence of Novel 116-Kilobase and 119-Kilobase Megaplasmids with Type VI Secretion
620 Systems. Genome Announc *4*.
621 Marasini, D., Karki, A.B., Bryant, J.M., Sheaff, R.J., and Fakhr, M.K. (2020). Molecular
622 characterization of megaplasmids encoding the type VI secretion system in Campylobacter
623 jejuni isolated from chicken livers and gizzards. Scientific reports *10*, 12514.
624 Marchesi, J.R., Cleary, D.W., and Clarke, S.C. (2017). The nasopharyngeal microbiome.
625 Emerging Topics in Life Sciences *1*, 297-312.
626 Mariano, G., Trunk, K., Williams, D.J., Monlezun, L., Strahl, H., Pitt, S.J., and Coulthurst, S.J.
627 (2019). A family of Type VI secretion system effector proteins that form ion-selective pores.
628 Nature communications *10*, 5484.
629 Marri, P.R., Paniscus, M., Weyand, N.J., Rendon, M.A., Calton, C.M., Hernandez, D.R., Higashi,
630 D.L., Sodergren, E., Weinstock, G.M., Rounsley, S.D.*, et al.* (2010). Genome sequencing reveals
631 widespread virulence gene exchange among human Neisseria species. PLoS One *5*, e11835.
632 Nadell, C.D., Drescher, K., and Foster, K.R. (2016). Spatial structure, cooperation and
633 competition in biofilms. Nature reviews Microbiology *14*, 589-600.
634 Nassif, X., Lowy, J., Stenberg, P., Ogaora, P., Ganji, A., and So, M. (1993). Antigenic Variation
635 of Pilin Regulates Adhesion of Neisseria-Meningitidis to Human Epithelial-Cells. Molecular
636 microbiology *8*, 719-725.

637 Oldewurtel, E.R., Kouzel, N., Dewenter, L., Henseler, K., and Maier, B. (2015). Differential
638 interaction forces govern bacterial sorting in early biofilms. eLife *4*.
639 Pissaridou, P., Allsopp, L.P., Wettstadt, S., Howard, S.A., Mavridou, D.A.I., and Filloux, A.
640 (2018). The Pseudomonas aeruginosa T6SS-VgrG1b spike is topped by a PAAR protein eliciting
641 DNA damage to bacterial competitors. Proceedings of the National Academy of Sciences of
642 the United States of America *115*, 12519-12524.
643 Ponisch, W., Eckenrode, K.B., Alzurqa, K., Nasrollahi, H., Weber, C., Zaburdaev, V., and Biais,
644 N. (2018). Pili mediated intercellular forces shape heterogeneous bacterial microcolonies
645 prior to multicellular differentiation. Scientific reports *8*, 16567.
646 Ramos-Sevillano, E., Wade, W.G., Mann, A., Gilbert, A., Lambkin-Williams, R., Killingley, B.,
647 Nguyen-Van-Tam, J.S., and Tang, C.M. (2019). The Effect of Influenza Virus on the Human
648 Oropharyngeal Microbiome. Clinical Infectious Diseases *68*, 1993-2002.
649 Ringel, P.D., Hu, D., and Basler, M. (2017). The Role of Type VI Secretion System Effectors in
650 Target Cell Lysis and Subsequent Horizontal Gene Transfer. Cell reports *21*, 3927-3940.
651 Roberts, M.C. (1989). Plasmids of Neisseria gonorrhoeae and other Neisseria species. Clin
652 Microbiol Rev *2 Suppl*, S18-23.
653 Round, J.L., and Mazmanian, S.K. (2009). The gut microbiota shapes intestinal immune
654 responses during health and disease. Nature reviews Immunology *9*, 313-323.
655 Russell, A.B., LeRoux, M., Hathazi, K., Agnello, D.M., Ishikawa, T., Wiggins, P.A., Wai, S.N., and
656 Mougous, J.D. (2013). Diverse type VI secretion phospholipases are functionally plastic
657 antibacterial effectors. Nature *496*, 508-512.
658 Russell, A.B., Wexler, A.G., Harding, B.N., Whitney, J.C., Bohn, A.J., Goo, Y.A., Tran, B.Q., Barry,
659 N.A., Zheng, H., Peterson, S.B*., et al.* (2014). A type VI secretion-related pathway in
660 Bacteroidetes mediates interbacterial antagonism. Cell host & microbe *16*, 227-236.

661 Sana, T.G., Flaugnatti, N., Lugo, K.A., Lam, L.H., Jacobson, A., Baylot, V., Durand, E., Journet,
662 L., Cascales, E., and Monack, D.M. (2016). Salmonella Typhimurium utilizes a T6SS-mediated
663 antibacterial weapon to establish in the host gut. Proceedings of the National Academy of
664 Sciences of the United States of America *113*, E5044-5051.
665 Schindelin, J., Arganda-Carreras, I., Frise, E., Kaynig, V., Longair, M., Pietzsch, T., Preibisch, S.,
666 Rueden, C., Saalfeld, S., Schmid, B.*, et al.* (2012). Fiji: an open-source platform for biological-
667 image analysis. Nature methods *9*, 676-682.
668 Sheikhi, R., Amin, M., Rostami, S., Shoja, S., and Ebrahimi, N. (2015). Oropharyngeal
669 Colonization With Neisseria lactamica, Other Nonpathogenic Neisseria Species and Moraxella
670 catarrhalis Among Young Healthy Children in Ahvaz, Iran. Jundishapur J Microb *8*.
671 Shneider, M.M., Buth, S.A., Ho, B.T., Basler, M., Mekalanos, J.J., and Leiman, P.G. (2013).
672 PAAR-repeat proteins sharpen and diversify the type VI secretion system spike. Nature *500*,
673 350-353.
674 Singh, P., Sharma, L., Kulothungan, S.R., Adkar, B.V., Prajapati, R.S., Ali, P.S., Krishnan, B., and
675 Varadarajan, R. (2013). Effect of signal peptide on stability and folding of Escherichia coli
676 thioredoxin. PLoS One *8*, e63442.
677 Smith, W.P.J., Vettiger, A., Winter, J., Ryser, T., Comstock, L.E., Basler, M., and Foster, K.R.
678 (2020). The evolution of the type VI secretion system as a disintegration weapon. Plos Biol *18*.
679 Sommer, F., and Bäckhed, F. (2013). The gut microbiota--masters of host development and
680 physiology. Nature reviews Microbiology *11*, 227-238.
681 Thévenaz, P., Ruttimann, U.E., and Unser, M. (1998). A pyramid approach to subpixel
682 registration based on intensity. IEEE transactions on image processing : a publication of the
683 IEEE Signal Processing Society *7*, 27-41.

684 Toska, J., Ho, B.T., and Mekalanos, J.J. (2018). Exopolysaccharide protects Vibrio cholerae
685 from exogenous attacks by the type 6 secretion system. Proceedings of the National Academy
686 of Sciences of the United States of America *115*, 7997-8002.
687 Unterweger, D., Miyata, S.T., Bachmann, V., Brooks, T.M., Mullins, T., Kostiuk, B., Provenzano,
688 D., and Pukatzki, S. (2014). The Vibrio cholerae type VI secretion system employs diverse
689 effector modules for intraspecific competition. Nature communications *5*, 3549.
690 Virji, M., Kayhty, H., Ferguson, D.J., Alexandrescu, C., Heckels, J.E., and Moxon, E.R. (1991).
691 The role of pili in the interactions of pathogenic Neisseria with cultured human endothelial
692 cells. Molecular microbiology *5*, 1831-1841.
693 Wade, J.J., and Graver, M.A. (2007). A fully defined, clear and protein-free liquid medium
694 permitting dense growth of Neisseria gonorrhoeae from very low inocula. FEMS microbiology
695 letters *273*, 35-37.
696 Whitney, J.C., Chou, S., Russell, A.B., Biboy, J., Gardiner, T.E., Ferrin, M.A., Brittnacher, M.,
697 Vollmer, W., and Mougous, J.D. (2013). Identification, structure, and function of a novel type
698 VI secretion peptidoglycan glycoside hydrolase effector-immunity pair. The Journal of
699 biological chemistry *288*, 26616-26624.
700 Wolcott, R., Costerton, J.W., Raoult, D., and Cutler, S.J. (2013). The polymicrobial nature of
701 biofilm infection. Clinical microbiology and infection : the official publication of the European
702 Society of Clinical Microbiology and Infectious Diseases *19*, 107-112.
703 Wörmann, M.E., Horien, C.L., Johnson, E., Liu, G., Aho, E., Tang, C.M., and Exley, R.M. (2016).
704 Neisseria cinerea isolates can adhere to human epithelial cells by type IV pilus-independent
705 mechanisms. Microbiology (Reading, England) *162*, 487-502.

706 Zöllner, R., Oldewurtel, E.R., Kouzel, N., and Maier, B. (2017). Phase and antigenic variation
707 govern competition dynamics through positioning in bacterial colonies. Scientific reports *7*,
708 12151.

709

710

711 **SUPPLEMENTARY FIGURES**

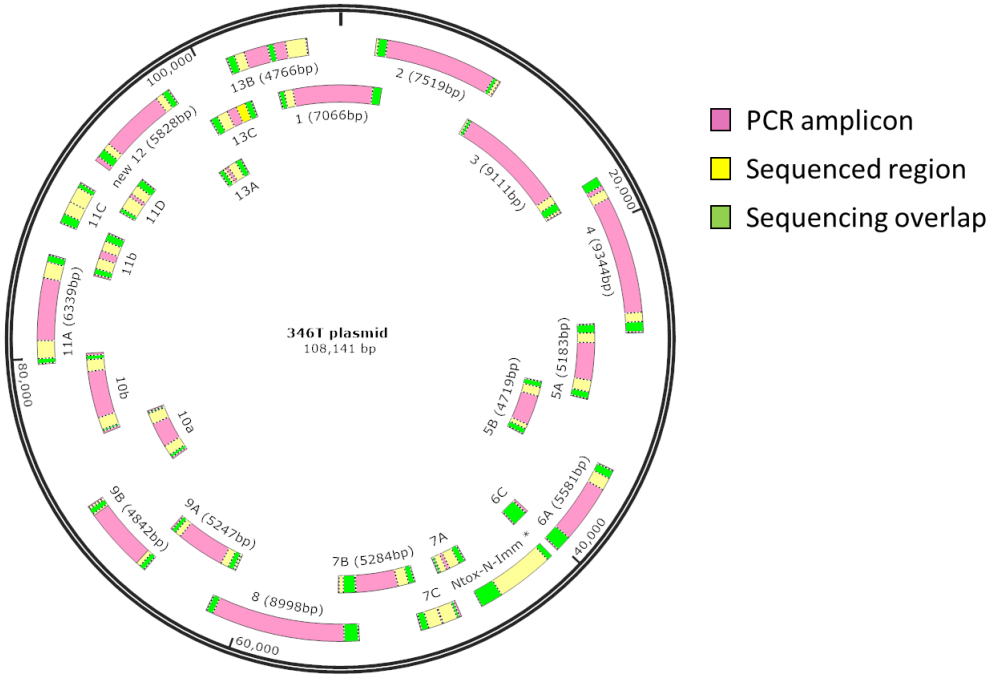

712

713 **Figure supplement 1. The *N. cinerea* 346T T6SS is encoded on a plasmid.**

714 Overlapping PCR and sequencing confirms extra-chromosomally closed circular DNA
715 fragment. A total of 25 PCR fragments (pink bars) were amplified from *N. cinerea* 346T
716 gDNA to confirm the plasmid predicted by PacBio whole-genome sequencing. Yellow shows
717 regions which were sequenced, and green indicates the overlapping amplified regions.

718

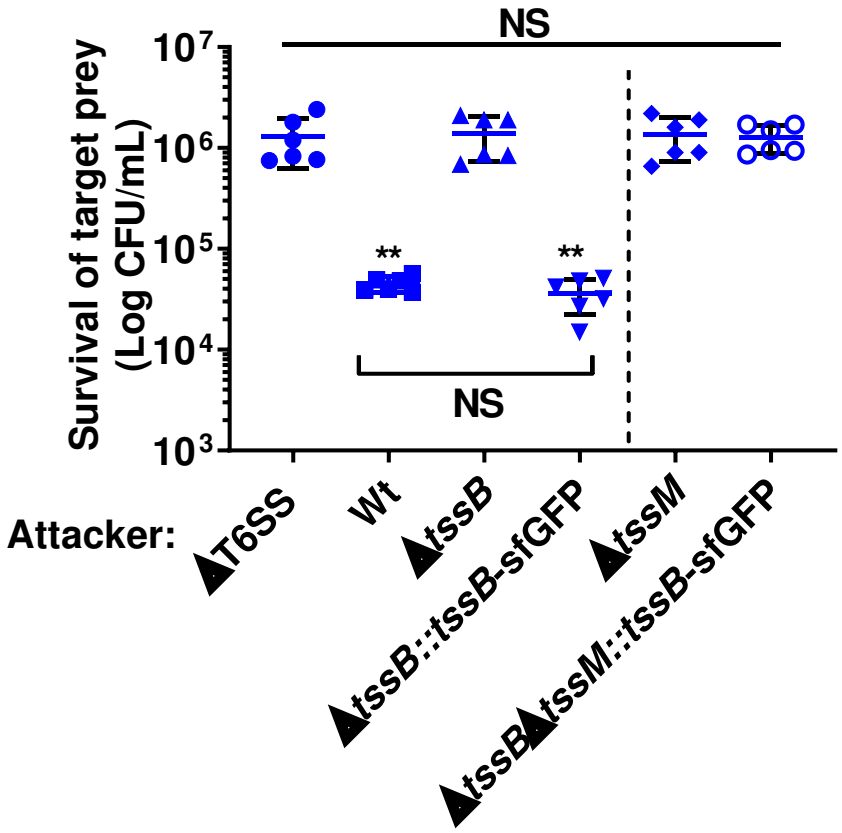

719

720 **Figure supplement 2.** ***N. cinerea*** **T6SS with a TssB C-terminal sfGFP fusion is functional and**

721 **activity is lost upon deletion of** ***tssM.*** Competition assay measuring the recovery of prey (*N.*

722 *meningitidis* 8013) after 4 h co-incubation with wild-type *N. cinerea* 346T (Wt) and specified

723 mutants at ratio of 100:1 (attacker:prey). Data shown are the mean ± SD of two

724 independent experiments: NS, not significant, **p < 0.005 using one-way ANOVA test for

725 multiple comparisons.

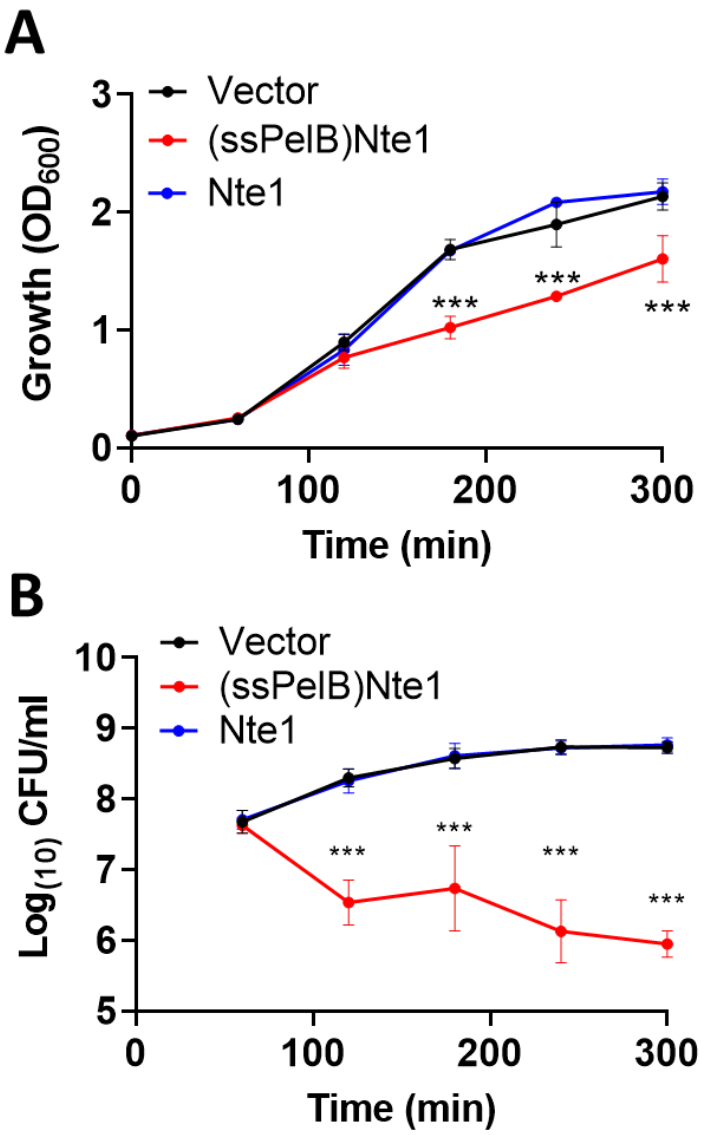

Figure supplement 3. *N cinerea* putative T6SS effector Nte1 requires a PelB signal sequence for toxicity in *E. coli.* (**A**) Toxicity of Nte1 with or without the PelB signal sequence (ssPelB) following expression in *E. coli*. Expression was induced with L-arabinose at 60 mins and bacterial growth was monitored by measuring the OD_{600} of cultures. A reduction on OD600 was only observed when Nte1 was expressed with ssPelB. (**B**) Samples collected after addition of arabinose were plated to media containing glucose to repress toxin expression and enumerated. Data, shown are mean ± SD of three independent experiments: NS, not significant, ***p < 0.0001, *p < 0.05 using two-way ANOVA test for multiple comparison.

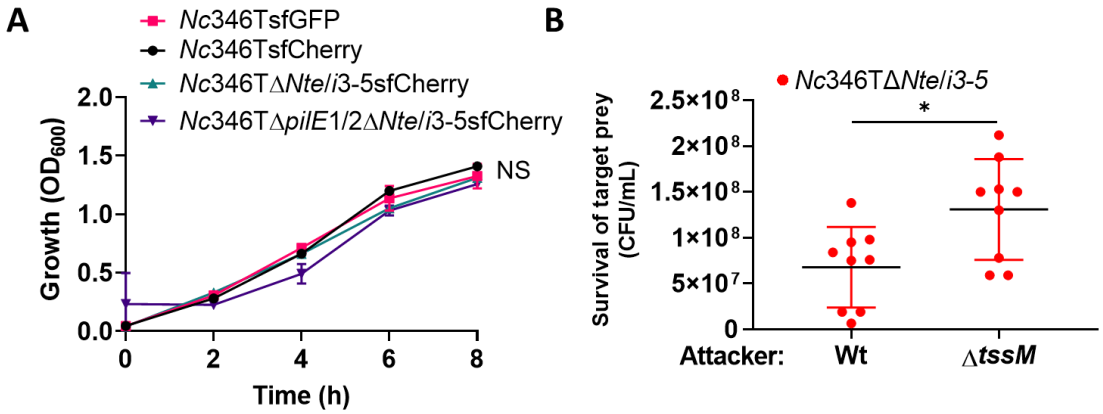

735

736 **Figure supplement 4. *N. cinerea* 346TΔ*nte*/*i3-5* has comparable growth to parent strain**

737 **and is susceptible to T6SS-killing by wild-type *N. cinerea* 346T.** (**A**) *N. cinerea* 346T strains

738 were grown in liquid BHI media for 8 h at 37˚C with 5% CO_2. Growth was monitored by

739 measuring the OD_{600} of cultures. Data are representative of two independent experiments:

740 NS, not significant, using two-way ANOVA test for multiple comparison. (**B**) Competition

741 assay measuring the recovery of the indicated *N. cinerea* 346TΔ*Nte*/*i3-5* mutant strain after

742 4 h of co-incubation wild-type *N. cinerea* 346T (Wt) or a *tssM*-deficient mutant (Δ*tssM*) at

743 ratio of 10:1 (attacker: prey). Data shown are the mean ± SD of three independent

744 experiments performed in triplicate: *$p < 0.05$ using unpaired two-tailed Student's t-test.

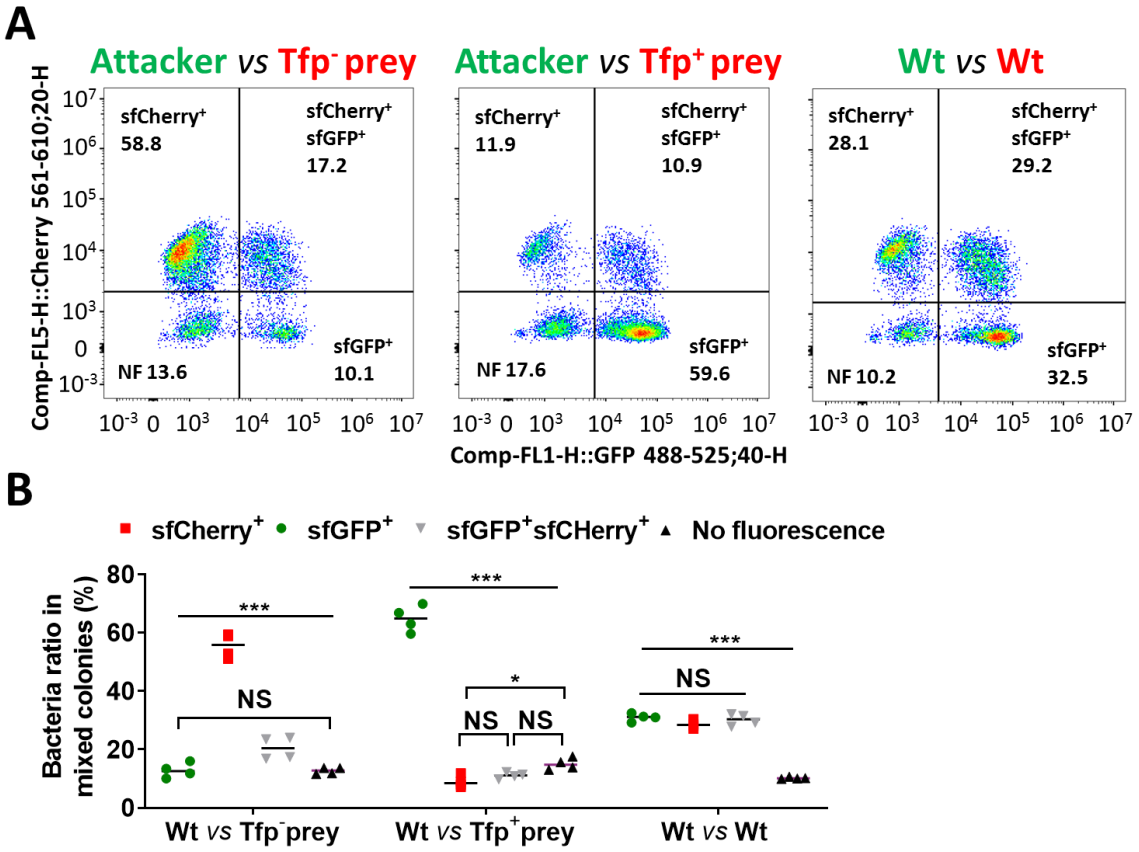

Figure supplement 5. Flow cytometry analysis of relative proportion of piliated and non-piliated prey in mixed colonies with T6SS-expressing piliated attacker strain. (A) Total bacteria in mixed colonies grown on agar plates were collected, fixed and analysed by Flow cytometry. Plots reveal shift in the dominant population after 24h growth. Plots are representative of two independent experiments with two technical repeats. **(B)** Histograms of data shown in panel a. When non-piliated, after 24 h the prey strain (red dots) dominates the population, despite being susceptible to T6SS-mediated attack (red prey 346TΔ*Nte*/*i3-5*Δ*pilE1/2_sfCherry* 56±4%, green attacker 346T_*gfp* 13±3%; $p < 0.0001$). Piliation of the prey reduces it to less than 10% of the population, and the attacker cells constitute the majority of the population (red prey 346TΔ*Nte*/*i3-5* 9±2%, green attacker 346T_*gfp* 65±5%, $p < 0.0001$). When the immunity of the prey is not compromised, piliated attacker and prey are detected in approximately equal proportions (red 346T_sfCherry 29±1%, green

346T_*gfp* 31±1%, $p = 0.58$. Data, shown are mean ± SD of two independent experiments: NS, not significant, * $p < 0.05$, ***$p < 0.0001$ using two-way ANOVA test for multiple comparison.

761 **SUPPLEMENTARY TABLES**

762 **Table supplement 1. Putative T6SS core components in *N. cinerea* 346T.**

763

Name	Protein Size (aa)	% aa (coverage) identity with *P. aeruginosa* PAO1	COG	Putative Localisation	Predicted Function
TssJ	215	35 (58)	COG3521	Outer membrane	Membrane complex
TssL	421	36 (91)	COG3455	Inner membrane	Membrane complex
TssM	1185	27 (93)	COG3523	Inner membrane	Membrane complex
TssK	447	37 (99)	COG3522	Inner membrane	Baseplate complex
TssF	640	33 (99)	COG3515	Inner membrane	Baseplate complex
TssG	346	37 (92)	COG3520	Inner membrane	Baseplate complex
TssE	170	37 (97)	COG3518	Cytoplasmic	Baseplate complex
TssA	355	28 (98)	COG3515	Cytoplasmic	Tail complex
TssB	172	70 (98)	COG3157	Cytoplasmic	Tail complex (sheath)
TssC	499	73 (97)	COG3517	Cytoplasmic	Tail complex (sheath)
ClpV	883	59 (98)	COG0542	Cytoplasmic	ATPase
Hcp	160	41 (100)	COG3157	Cytoplasmic/Inner membrane	Tail complex (Hcp tube)
VgrG	757	35 (99)	COG3501	Inner membrane	Spike

764

765

766 **Table supplement 2. Bacterial strains used in this study.**

Strains or plasmids	Description	Ref/ Source
Neisseria cinerea		
CCUG346T (346T)	wild-type *N. cinerea*	Bennett et al., 2012
CCUG27178A (27178A)	wild-type *N. cinerea*	Bennett et al., 2012
346T_sfGFP	346T with chromosomally integrated *sfGfp*; Ery^R	Wörmann et al., 2016
346T_sfCherry	346T with chromosomally integrated *sfCherry*; Ery^R	This study
27178A_sfCherry	27178 with chromosomally integrated *sfCherry*; $Spec^R$	This study
346TΔT6SS	346T with insertion-deletion of *tssC – vgrG* region; Ery^R	This study
346TΔ*tssB*	346T with insertion-deletion of *tssB*; Ery^R	This study
346TΔ*tssB::tssBsfGFP*	346T with insertion-deletion of native *tssB* and ectopic chromosomal insertion of *tssB-sfGFP* fusion; $Spec^R$ Ery^R	This study
346TΔ*tssM*	346T with insertion-deletion of *tssM*; Tet^R	This study
346TΔ*tssB*Δ*tssM::tssB*-sfGFP	346T with insertion-deletion of native *tssB* and *tssM* and ectopic chromosomal insertion of *tssB-sfGFP* fusion; $Spec^R$ Ery^R Tet^R	This study
346TΔ*nte/i3-5_sfCherry*	346T with insertion-deletion of *nte/i3-5* region and ectopic chromosomal insertion of *sfCherry*; $Spec^R$ Ery^R	This study
346TΔ*nte/i3-5*Δ*pilE1/2_sfCherry*	346T with insertion-deletion of *nte/i3-5* region; ectopic chromosomal insertion of *sfCherry*; insertion-deletion of *pilE1* and *pilE*2; kan^R,$Spec^R$ Ery^R	This study
Neisseria meningitidis		
8013	*N. meningitidis* wild-type	Rusniok et al., 2009
MC58	*N. meningitidis* wild-type	Tettelin et al., 2000
S3	*N. meningitidis* wild-type	Uria et al., 2008
MC58Δ*siaD*	deletion mutagenesis, *NEIS0051*; Kan^R	Virji et al., 1995
Neisseria gonorrhoeae		
FA1090 pGCC4	FA1090 with chromosomally integrated plasmid pGCC4; Ery^R	Mehr and Seifert, 1997
Escherichia coli		
Dh5α	*Cloning strain*	Lab collection
Dh5α pNCC1-Spec	Dh5α *with pNCC1[2] $Spec^R$ plasmid*	This study

Dh5α pNCC1-Spec-sfGFP	Dh5α with pNCC1-Spec with sfGFP insert;	This study
Dh5α pNCC101-Spec-sfCherry	DH5α with plasmid pNCC101+sfCherry insert. $Spec^R$	Lab collection
Dh5α pUC19::Δ*tssB*	DH5α with pUC19::Δ*tssB* deletion construct; $Carb^R$ Ery^R	This study
Dh5α pUC19::Δ*tssM*	DH5α with pUC19::Δ*tssM* deletion construct; $Carb^R$ Tet^R	This study
Dh5α pUC19::ΔT6SS	DH5α with pUC19::Δ*tssC-vgrG* locus deletion construct; $Carb^R$ Ery^R	This study
Dh5αpUC19:: Δ*nte3*Δ*nte4*n*Nte5*	DH5α with pUC19::Δ*nte3*Δ*nte4*n*Nte5 region* including respective immunity genes deletion construct; $Carb^R$ Ery^R	This study
B834 pET28a	*B834 with pET28a IPTG-inducible expression vector, Amp^R*	Lab collection
Dh5α pET28a-His-3C-Hcp	Dh5α with pET28a vector for IPTG inducible expression of Nc 346T Hcp with N-terminal cleavable HIS tag. *Amp^R*	This study
B834 pET28a-His-3C-Hcp	B834 expression strain, with pET28a vector for IPTG inducible expression of Nc 346T Hcp with N-terminal cleavable HIS tag. *Amp^R*	This study
Dh5α pBAD33	Dh5α with pBAD33 vector for *Arabinose-inducible expression, Cm^R*	Lab collection
Dh5α pBAD33::(ssPelB)Nte1-His	Dh5α with pBAD33 encoding *Nte1 with N-terminal PelB leader peptide and C-terminal his-tag under arabinose-inducible promoter control; Cm^R*	This study
Dh5α pBAD33:: (ssPelB)Nte1+Nti1	Dh5α with pBAD33 encoding *Nte1 with N-terminal PelB leader peptide and C-terminal his-tag plus Nti, under arabinose-inducible promoter control; Cm^R*	This study
Dh5α pBAD33::Nte1-His	Dh5α with pBAD33 encoding *Nte1 with N-terminal his-tag under arabinose-inducible promoter control; Cm^R*	This study
Dh5α pBAD33::Nte2	Dh5α with pBAD33 encoding *Nte2 under arabinose-inducible promoter control; Cm^R*	This study
Dh5α pBAD33::Nte2+Nti2	Dh5α with pBAD33 encoding *Nte2+Nti2 under arabinose-inducible promoter control; Cm^R*	This study
Dh5α pBAD33::Nte3	Dh5α with pBAD33 encoding *Nte3 under arabinose-inducible promoter control; Cm^R*	This study
Dh5α pBAD33::Nte3+Nti3	Dh5α with pBAD33 encoding *Nte3+Nti3 under arabinose-inducible promoter control; Cm^R*	This study
Dh5α pBAD33::Nte4	Dh5α with pBAD33 encoding *Nte4 under arabinose-inducible promoter control; Cm^R*	This study
Dh5α pBAD33::Nte4+Nti4	Dh5α with pBAD33 encoding *Nte4+Nti4 under arabinose-inducible promoter control; Cm^R*	This study
Dh5α pBAD33::Nte5	Dh5α with pBAD33 encoding *Nte5 under arabinose-inducible promoter control; Cm^R*	This study
Dh5α pBAD33::Nte5+Nti5	Dh5α with pBAD33 encoding *Nte5+Nti5 under arabinose-inducible promoter control; Cm^R*	This study
Dh5α pBAD33::$Nte6^{R1300S}$	Dh5α with pBAD33 encoding *$Nte6^{R1300S}$ under arabinose-inducible promoter control; Cm^R*	This study
Dh5α pBAD33::Nte6+Nti6	Dh5α with pBAD33 encoding *Nte6+Nit6 under arabinose-inducible promoter control; Cm^R*	This study

767

768 **Table supplement 3. Primers used in this study.**

Name	Sequence (5´-3´)	Use
T6SSdel-1	CGAAAAGTGCCACCTGACGTATGACTGAAAAGC AATTAGATATC	Deletion of *tssC-vgrG* locus
T6SSdel-2	GTTAAATTTAAGGATAAGAAACGTGGCAG	Deletion of *tssC-vgrG* locus
T6SSdel-3	TTTCTTATCCTTAAATTTAACGATCACTCATCATG	Deletion of *tssC-vgrG* locus
T6SSdel-4	ACTCAAACATTTACTTATTAAATAATTTATAGCTA TTGAAAAG	Deletion of *tssC-vgrG* locus
T6SSdel-5	TTAATAAGTAAATGTTTGAGTTGCAGAACTTTAC	Deletion of *tssC-vgrG* locus
T6SSdel-6	GATAATAATGGTTTCTTAGACGTGCCGTTCCAAT AGGCCATAG	Deletion of *tssC-vgrG* locus
T6SSdel-conf-F	CCTAAAGCGGCTTCCAAAGACG	Confirmation of *tssC-vgrG* locus deletion
T6SSdel-conf-R	CCATGCCGGTAAAGGTCAGT	Confirmation of *tssC-vgrG* locus deletion
TssBdel-1	GATCCTCTAGAGTCGACCTGCAGGCATGCACTTA CCCTGATCCACAAAGCC	Deletion of *tssB*
TssBdel-2	ATTCAATGACCTTTAAATGATAAAAGTTGT	Deletion of *tssB*
TssBdel-3	ACAACTTTTATCATTTAAAGGTCATTGAATATGA ACGAGAAAAATATAAAACACAGTC	Deletion of *tssB*
TssBdel-4	TTACTTATTAAATAATTTATAGCTATTGAAAAGA GATAAGAATTG	Deletion of *tssB*
TssBdel-5	TATAAATTATTTAATAAGTAAGCTTCCAAAGACG AGCAGTAA	Deletion of *tssB*
TssBdel-6	CAGGAAACAGCTATGACCATGATTACGCCTAAGT TGCGGGCAACTTCTT	Deletion of *tssB*
TssBdel-conf-F	ATAGAAACCTACTTTTTCGGAAAGC	Confirmation of *tssB* deletion
TssBdel-conf-R	TTACTTATTAAATAATTTATAGCTATTGAAAAGA GATAAGAATTG	Confirmation of *tssB* deletion
TssMdel-1	GATCCTCTAGAGTCGACCTGCAGGCATGCAACCC TGTCTTGGCTAGAGTC	Deletion of *tssM*
TssMdel-2	ATTTGTTTTTCCGTATCAATCCAATTTCA	Deletion of *tssM*
TssMdel-3	ATTGGATTGATACGGAAAAACAAATATGAAAAT TATTAATATTGGAGTTTTAGCTCATGTT	Deletion of *tssM*
TssMdel-4	CTAAGTTATTTTATTGAACATATATCGTACTTTAT CTATCCG	Deletion of *tssM*
TssMdel-5	AAGTACGATATATGTTCAATAAAATAACTTAGAA TAAATTAAGGAATTTTCAGTGCATTTGAAG	Deletion of *tssM*
TssMdel-6	CAGGAAACAGCTATGACCATGATTACGCCGGCA ATATCTAGAACGGATTTATCG	Deletion of *tssM*
TssMdel-Conf-F	AGGACTTCCAAGATAGAAGTACGG	Confirmation of *tssM* deletion
TssMdel-Conf-R	AAAGCCCCTTGTACGATAGC	Confirmation of *tssM* deletion
Nte345del-1	GATCCTCTAGAGTCGACCTGCAGGCATGCAGAC CTTCATGCTGACTAGTGAT	Deletion of *Nte3-Nte5* locus
Nte345del-2	GAAGTGTTGGATGAACTTTTTCTATG	Deletion of *Nte3-Nte5* locus
Nte345del-3	CATAGAAAAAGTTCATCCAACACTTCTTAAATTTA ACGATCACTCATCATGT	Deletion of *Nte3-Nte5* locus
Nte345del-4	TTACTTATTAAATAATTTATAGCTATTG	Deletion of *Nte3-Nte5* locus
Nte345del-5	CAATAGCTATAAATTATTTAATAAGTAAAATAAG AAACTGTAAACACAGTGTG	Deletion of *Nte3-Nte5* locus
Nte345del-6	CAGGAAACAGCTATGACCATGATTACGCCAGTTT AACTGTTCGGAAAGGGTGT	Deletion of *Nte3-Nte5* locus

Nte345del-conf-F	GTTTTCGTTGGTGAGGACGG	Confirmation of *Nte3-Nte5* locus deletion
Nte345del-conf-R	CTACTTATAATCCAAATATTTTATTGAACAGAGAAC	Confirmation of *Nte3-Nte5* locus deletion
TssBsfGFP1	CATGATTACGAATTCCCGGATTAATTAAAATGTCACGAAACAAATCATCCGG	*tssB* amplification to fuse with sfGFP and clone into pNCC1-spec
TssBsfGFP2	CTGCTCGTCTTTGGAAGC	*tssB* amplification to fuse with sfGFP and clone into pNCC1-spec
TssBsfGFP3	GCTTCCAAAGACGAGCAGGCAGCAGCAGGTGGTGGTAGCAAAGGAGAAGAACTTTTCAC	sfGFP amplification and addition of DNA linker to fuse with *tssB* and clone into pNCC1-spec
TssBsfGFP4	GATCCTCTAGAGTCGACCTGCAGGCATGCTCATTTGTAGAGCTCATCCATGC	sfGFP amplification and addition of DNA linker to fuse with *tssB* and clone into pNCC1-spec
sfGFP-Prom-F	TGACCCGGGTCATTTGTAGAGCTCATCCATGCC	sfGFP amplification from pNCC1-sfGFP to clone into pNCC1-spec
sfGFP-Prom-R	TGAAAGCTTTTGACAGCTAGCTCAGTCCTAGGTATAATGCTAGCCCAACATGTTACACAATAATGGAGTAATGAACATATGAGCAAAGGAGAAGAACT	sfGFP amplification from pNCC1-sfGFP to clone into pNCC1-spec
pGib-RBS-Nte2-F	GATCCTCTAGAGTCGACCTGCAGGCATGCAAAGAAGGAGATATACCATGGCATTCAATAAAATCGCCC	*Nte2* amplification and addition of RBS to clone into pBAD33
pGib-RBS-Nte2-R	AAAATCTTCTCTCATCCGCCAAAACAGCCATCATTTTTCCTATTGTTACATTTATCCT	*Nte2* amplification and addition of RBS to clone into pBAD33
pGib-RBS-Nti2-R	AAAATCTTCTCTCATCCGCCAAAACAGCCATTATTCAAATTTCTTTAGCAGTATTTTTCT	*Nte2* and *Nti2* amplification plus addition of RBS to clone into pBAD33
pGib-RBS-Nte3-F	GATCCTCTAGAGTCGACCTGCAGGCATGCAAAGAAGGAGATATACCATGGCCTCTTTCGGTAAC	*Nte3* amplification and addition of RBS to clone into pBAD33
pGib-RBS-Nte3-R	AAAATCTTCTCTCATCCGCCAAAACAGCCATCATTTAATACCTCTTCTTGATAATTCTTT	*Nte3* amplification and addition of RBS to clone into pBAD33
pGib-RBS-Nti3-R	AAAATCTTCTCTCATCCGCCAAAACAGCCACTATTCACCCAACAATGTTTCT	*Nte3* and *Nti3* amplification plus addition of RBS to clone into pBAD33
PGIB-RBS-NTE4-F	GATCCTCTAGAGTCGACCTGCAGGCATGCAAAGAAGGAGATATACCATGGTCGAACACAACCAG	*Nte4* amplification and addition of RBS to clone into pBAD33
pGib-RBS-Nte4-R	AAAATCTTCTCTCATCCGCCAAAACAGCCATTAAATTATTGGAAGATTTTTACAACCA	*Nte4* amplification and addition of RBS to clone into pBAD33
pGib-RBS-Nti4-R	AAAATCTTCTCTCATCCGCCAAAACAGCCATTACGCTTTTAAATTCCGGTG	*Nte4* and *Nti4* amplification plus addition of RBS to clone into pBAD33
pGib-RBS-Nte5-F	GATCCTCTAGAGTCGACCTGCAGGCATGCAAAGAAGGAGATATACCATGGGTCGTCTGAAAAGC	*Nte5* amplification and addition of RBS to clone into pBAD33
pGib-RBS-Nte5-R	AAAATCTTCTCTCATCCGCCAAAACAGCCACTAATCTAATCGTTTGGGCG	*Nte5* amplification and addition of RBS to clone into pBAD33
pGib-RBS-Nti5-R	AAAATCTTCTCTCATCCGCCAAAACAGCCATTAATCCCAATAACTGTCTAAATTGT	*Nte5* and *Nti5* amplification plus addition of RBS to clone into pBAD33
pGib-RBS-Nte6-F	GATCCTCTAGAGTCGACCTGCAGGCATGCAAAGAAGGAGATATACCATGGCCTCTTTCGGTAAC	*Nte6* amplification and addition of RBS to clone into pBAD33
pGib-RBS-Nte6-R	AAAATCTTCTCTCATCCGCCAAAACAGCCACTATTATCTAGGAACAATCTGATTAATTATTCC	*Nte6* amplification and addition of RBS to clone into pBAD33
pGib-RBS-Nti6-R	AAAATCTTCTCTCATCCGCCAAAACAGCCATTAAATTTCCTCTAGTTTTTCTTTCATC	*Nte6* and *Nti6* amplification plus addition of RBS to clone into pBAD33

CE043-F	GGCCGGTCTAGAAAGAAGGAGATATACCATGAAATACCTGCTGCCGACCGCTGCTGCTGGTCTGCTGCTCCTCGC	Addition of *5' PelB leader peptide and 3' 6xHIS-tag* to PLA2 domain to clone into pBAD33
CE044-F	GGTCTGCTGCTCCTCGCTGCCCAGCCGGCGATGGCCATGGGGGGAAGTAATTTTTATGCGTTTGCA	PLA2 domain amplification and addition of *5' PelB leader peptide*
CE046-R	CCGGCCGCATGCCTAGTGATGGTGATGGTGATGCCTATGATTTTTAGAC	Addition of *3' 6xHIS-tag* to PLA2 domain with or without *5' PelB leader peptide* to clone into pBAD33
CE047-R	GATGCCTATGATTTTTAGACGTTTTTTTAATTGTTTTATCG	PLA2 domain amplification with or without addition of *5' PelB leader peptide*
CE048-R	CCGGCCGCATGCCTAGTGATGGTGATGGTGATGATTAAGTTTGGATAGTTTGAAAATTTTTTTAAGCTTATATATAAG	PLA2 domain amplification with or without a *5' PelB leader peptide and amplification of Nti1 adding a 3' 6xHIS-tag to clone into pBAD33*
CE083-F	GGCCGGTCTAGAAAGAAGGAGATATACCATGGGGGGAAGTAATTTTTATGCGTTTGCA	PLA2 domain amplification and addition of *3' 6xHIS-tag* to clone into pBAD33
MW312	TATAAGGAGGAACATATGGAATACATGTTATAATAACTATAAC	Spectinomycin cassette amplification from pDG1728 to clone into pNCC1
MW313	GTATTCCATATGTTCCTCCTTATAAAATTAGTATAATTATAG	pNCC1 plasmid backbone amplification
MW314	GCATCCCTTAACGACGTCAATTGAAAAAAGTGTTTCCACC	Spectinomycin cassette amplification from pDG1728 to clone into pNCC1
MW315	TCAATTGACGTCGTTAAGGGATGCATAAACTGCATCCCTTAAC	pNCC1 plasmid backbone amplification

769

770 **SUPPLEMENTARY MOVIES LEGENDS**

771

772 **Movie supplement 1.** Visualisation of *N. cinerea* T6SS contraction.

773 *N. cinerea* 346TΔ*tssB::tssBsfGFP* (green) and prey cells *N. cinerea* 27178A_*sfCherry* (red)

774 were mixed at a ratio of 1:1 and spotted on a 1% agarose PBS pad supplemented with 0.1

775 mM IPTG. The cells were imaged for 12 seconds with a rate of 1 image per second.

776

777 **Movie supplement 2.** Visualisation of *N. cinerea* T6SS foci.

778 *N. cinerea* 346TΔ*tssB*::*tssB*sfGFP (green) or *N. cinerea* 346T*ΔtssBΔtssM::tssBsfGFP* (green) and

779 prey cells *N. cinerea* 27178A_*sfCherry* (red) were mixed at a ratio of 1:1 and spotted on a PBS

780 1% agarose pad supplemented with 0.1 mM IPTG. The cells were imaged for 200 seconds with

781 a rate of one image per 10 seconds.

782

783 **Movie supplement 3.** *N. cinerea* T6SS elicits prey lysis.

784 *N. cinerea* 346TΔ*tssB*::*tssB*sfGFP (green) and *N. cinerea* 27178A_*sfCherry* (red) were mixed

785 at a ratio of 1:1 and spotted onto agarose padS supplemented with 0.1 mM IPTG and the

786 cell-impermeable DNA stain SYTOX Blue (0.5 µM) as an indicator for loss of membrane

787 integrity. The cells were imaged for 10 min with an image taken every 10 seconds.

788

789 **Movie supplement 4.** Growing edge of colonies with a piliated attacker *N. cinerea* 346T_*gfp*,

790 (green) and non-piliated prey 346TΔ*nte*/*i3-5*Δ*pilE1*/*2_sfCherry* (red).

791 Strains were spotted at a ratio of 1:1. Colonies were imaged every 2 h between 4 and 16 h

792 post inoculation. Over time a population of non-piliated prey segregates to the edge, escape

793 T6SS assault and dominates the growing colony.

794

795 **Movie supplement 5.** Growing edge of colonies with a piliated attacker *N. cinerea* 346T_*gfp*,

796 (green) and piliated prey 346TΔ*nte*/*i3-5*_*sfCherry* (red).

797 Strains were spotted at a ratio of 1:1. Colonies were imaged every 2 h between 4 and 16 h

798 post inoculation. Over time the T6SS expressing strain dominates the colony.

799

800 **Movie supplement 6.** Growing edge of colonies with two wild-type strains. *N. cinerea*

801 346T_*gfp* (green) and *N. cinerea* 346T_*sfCherry* (red).

802 Strains were spotted at a ratio of 1:1. Colonies were imaged between 4 and 16 h post

803 inoculation. Images obtained every 2 h. No dominance of either strain is observed.

804